DETECTION OF ALGAL BLOOMS IN LAKES

Using Sentinel-1 C-band SAR Images

Geetika Rathee

06-02-2017

WAGENINGEN UNIVERSITY
WAGENINGEN UR

Detection of Algal Blooms in Lakes Using Sentinel-1 C-band SAR Images

Geetika Rathee
Registration Number: 900530 680 010

Supervisors:

Dr. Jan Clevers (WUR)
Dr. Steef Peters (Water Insight)
Dr. Annelies Hommersom (Water Insight)
Dr. Johannes Reiche (WUR)

A thesis submitted in partial fulfilment of the degree of Master of Science
at Wageningen University and Research,
The Netherlands.

06 February 2017
Wageningen, The Netherlands

Preface

This dissertation is submitted for the fulfillment of the degree of Master of Science in Geo-Information Science at Wageningen University. The research herein is original, except where acknowledgment and references are made. It is an unpublished and independent work by the author. The work has been performed under the primary supervision of Dr. Jan Clevers in the Laboratory of Geo-Information Science and Remote Sensing, WUR and Dr. Steef Peters, director at Water Insight BV, Wageningen. The research is co-supervised by Dr. Annelies Hommersom in Water Insight and Dr. Johannes Reiche in the Laboratory of Geo-Information Science and Remote Sensing, WUR.

Geetika Rathee
06 February 2017
Wageningen

Foreword

This study was an interesting and fulfilling experience for me. The key subject of study, algae are the primary producer of energy and hold great significance for life in water and environment at large. During the study, I was enamoured by the immensity of life flourishing in the water bodies. The work entailed many challenges for me. At the beginning of the thesis, I did not have scientific understanding of water systems and algae growth dynamics. Additionally, the C-SAR images turned out to be more complicated to understand than optical images. At that time, I was only aware of the basics of microwave remote sensing. Fortunately, with time, my interest in the subject also grew and I was able to overcome difficulties slowly and steadily. This research opened new learning avenues for me. Not only did I push myself into uncharted territories; I also learnt the scientific approach to tackle unknown subjects in the field of remote sensing. This could not have been possible without all the help, support and confidence I received from my friends, university faculty and my colleagues at Water Insight. All of them were always ready to help and welcomed my questions with smile.

First of all, I want to thank my supervisors for allowing me to work at my pace and pushing me to reach my full potential. I received valuable feedback from them every step of the way. This helped in streamlining the research and in writing of this report. I would like to also thank my co-supervisors Annelies and Johannes, who gave me confidence in my work and critical feedback on parts of research in their areas of expertise. I also like to thank Mr. Jannes, who provided expert knowledge on the activities of lake Paterswoldsemeer. I am also thankful to Dr. Giacomo and Dr. Bresciani for giving me time to discuss parts of my research. Their interest and appreciation means a lot to me. Also, Dr. Giacomo provided me critical information about sensing algae in SAR image. I want to thank all my dear friends for bearing with my emotional self and accompanying me in times of stress and disappointments. Finally, I want to thank my boyfriend Ravi and my mother for providing moral support and encouragement.

Geetika Rathee
06 February 2017
Wageningen

Summary

The beginning of summer marks an onset of exponential growth of algae in lakes of the northern parts of the world. Eutrophication is a naturally occurring phenomenon but it has undergone drastic change, in terms of the intensity of algal blooms and their species composition. Algal blooms are lasting longer and occur more often, and in some lakes they are dominated by potentially toxic algae. Toxic algal blooms put a heavy toll on environment's health and economy sustained by the lake.

Over the last decade, optical remote sensing has become a popular tool for sensing, monitoring and developing better understanding of the state of lakes. However, as the situation becomes more hazardous for people living in the vicinity of lakes suffering from toxic algal blooms, optical images alone may not be sufficient. Optical remote sensing is hindered by clouds. For regions with frequent cloud cover, this means loss of data, which derails the purpose of sensing.

Microwave remote sensing, which was mostly a tool to study atmosphere and planetary surfaces in the twentieth century, is increasingly being used to understand our planet, Earth. The European Space Agency launched two radar imaging sister satellites (Sentinel-1a & 1b) in 2014 and 2016, which are sensing the Earth with an improved spatial and temporal resolution. The C-band Synthetic Aperture Radar sensor mounted on the two satellites is capable of sensing the Earth uninterruptedly, irrespective of weather conditions.

One of the major existing applications of radar imaging has been the monitoring of oil spills in seas and oceans. Spilled oil reduces the strength of the signal received from the ocean/sea surface and appears as dampened regions in the image. Interestingly, the automated algorithms meant to locate oil spills produced false oil spill alarms from the presence of algal blooms. This broadened the use of radar imaging towards understanding algal phenology across oceans. Studies on sensing algae infestation in water bodies show a negative correlation between indices indicative of algae concentration from optical imageries and backscatter signal in radar image. However, most existing studies on monitoring algae using radar are performed for seas and oceans and not for smaller water bodies such as lakes. The focus of this study is to explore Sentinel-1a C-SAR data to locate algal infestation in lakes using in-situ data for

validation. The C-SAR images are analyzed for change in the water surface signal during blooms.

Two study sites, lake Utah and lake Paterswoldsemeer, which suffered from blooms of blue-green algae during the summer of 2016, are studied to explore visibility of algae in radar images. First, factors that affect radar signals are identified by analyzing the data from the first study site - lake Utah. It is 370 km^2 in area and nearly 90 percent of the area suffered from blooms. Then, these are tested for lake Paterswoldsemeer to check if in this lake similar changes in radar signals from algae infestation can be observed. The lake is about 2 km^2 in area and mainly had sub-surface bloom of width more than 100 m.

It is observed that the relation of the radar signal with wind conditions was positive for both sites for times when they did not suffer from algal blooms. It is found that the two lakes did not show similar changes in backscatter during the time of algae infestation. Lake Utah showed attenuation in signal and was resistant to turbulence in the regions that suffered from an algae bloom. For lake Paterswoldsemeer, the regions suffering from an algal bloom did not confirm results of the Utah case study. It is hypothesized that size of lake is a crucial element in judging the success of detecting algae in lakes. This is because the size usually is an indicator of the length of fetch. Long fetch allows for the development of stabilized wind stress which enhances the visibility of algae in lakes.

There is need for more systematic and bigger research on effects of local factors and topography in changing the radar signal using more extensive in-situ data or integration of data from multiple sources. Knowledge of various factors acting on the lake is crucial to isolate probable agents of change in the radar signal other than algae. This is especially true for lakes, which are smaller and interconnected with other water channels, located around unique topography and witness heavy traffic load.

Keywords: Algae, lakes, inland water-bodies, radar, C-SAR, sensing, Sentinel-1, blue-green algae, scum

Glossary

ASI: Italian Space Agency
C-SAR: C-band Synthetic Aperture Radar
CAST: China Academy of Space Technology
CMOD: C-band Radar Sea Echo Model
DEM: Digital Elevation Model
DLR: Deutsches Zentrum für Luft- und Raumfahrt
EO: Earth Observation
ESA: European Space Agency
EUMETSAT: European Organisation for the
ISRO: Indian Space and Research Organization
JAXA: Japan Aerospace Exploration Agency
NASA: National Aeronautics and Space Administration
SAR: Synthetic Aperture Radar
SRTM: Shuttle Radar Topography Mission

List of Figures

List of Tables

Table of Contents

Chapter 1: Introduction

Algae infestation in freshwater lakes has become problematic in the temperate zone due to increase in the intensity and change in the composition of algal blooms. Scientists in the field of remote sensing are working towards improving methods to measure growth and distribution of algae in lakes. In this study, the use of C-band radar satellite images is explored for detecting algae in lakes. The use of radar images for monitoring lakes is very challenging for several reasons. The low spatial resolution of radar images of the twentieth century and low backscatter signal received from a water surface are among the key reasons. Recent advancements in radar imaging (especially the launch of Sentinel-1 in 2014) is expected to lead to the improvement in spatial and temporal resolution (Torres et al., 2012). Sentinel-1 C-band SAR images are explored to locate factors that affects the visibility of algae in two lakes in the northern hemisphere, Lake Utah and Lake Paterswoldsemeer.

1. 1 Context and background

The need of monitoring: Global warming and increasing frequency of heat waves has led to frequent outbreaks of algal blooms in inland water bodies (Paerl & Huisman, 2008). Algal blooms are an unpleasant sight and hinder various recreational and economic activities sustained by a water body such as boating, fishing, etc. (Álvarez et al., 2008). Increase in anthropogenic loading of nutrients (the process known as eutrophication) has led to an increase in the occurrence of toxic algae, the blue-green algae (or cyanobacteria) in coastal and inland water bodies (Sellner, 2003; Heisler, 2008; Anderson, Glibert & Burkholder, 2002). A mature blue-green algae bloom often surfaces atop as a layer of scum containing high concentrations of toxins (Medrano, 2014). Contact to these toxins poses a direct health risk to both humans and animals (Chorus & Bartram, 1999). Therefore, the monitoring of algae concentration in lakes has become a topic of interest to management and science (Meriluoto & Codd, 2005). While scientists are occupied with furthering the understanding of biological and physical growth dynamics of various algae species, water managers are interested in monitoring the state of lakes to be able to warn the public in time.

Current monitoring systems for lakes: In-situ data is most widely used dataset for monitoring inland water bodies such as lakes and canals. The European directives, "Water Framework Directive" and the "Bathing Water Directive" demand water authorities to monitor water bodies using at the least, traditional sampling techniques (Hering et al., 2010). Some European water management authorities (for example in Finland) are using in-situ data with satellite imagery to monitor the state of their water bodies (GLaSS D. 5.7, 2015). Satellite data is cost effective, frequent and provides a full spatial coverage at a coarse level. It allows for trend detection in space and time. In-situ data on the other hand, produce highly accurate, precise and in depth information on the state of a location at a point in time. Although an extensive in-situ data coverage may be more desirable, cost and maintenance often limit the in-situ coverage of a water body. Both sets of data provide a different truth about the state and the integration of in-situ information with large spatial datasets has been very useful in enhancing our understanding of the environment (Reynolds et al., 2002; Gardner, Mishonov, & Richardson, 2006). Synthesis of satellite data with other sources of information has potential of improving the management by enhancing our understanding of algae growth in water bodies (Miller et al., 2006; Duan, Ma & Hu, 2012).

Remote sensing of algae: Algae bear properties, which can be exploited to detect them with remote sensing. Most algae have characteristic pigments, such as phycocyanin, phycoerythrin and chlorophyll-a that give them colors like blue, green, red, yellow or even brown (Racault et al., 2012). Some algae show affinity to certain weather conditions (Bricaud, Bosc & Antoine, 2002). Algal blooms in oceans and seas can be detected using remote optical, thermal and microwave sensors (Barale, Gower & Alberotanza, 2010). Different sensors (data-types) provide different information about blooms and have their own advantages and disadvantages. Most research in the past decade have focused on the use of optical properties for remote sensing of blooms (Racault et al., 2012). Optical sensors use color of their pigments to identify a bloom event (Ishizaka, Sathyendranath & Platt, 2010). Researchers are mapping blooms using optical imagery in marine, lacustrine and lagoonal environments using site specific semi-empirical algorithms (Zimba & Gitelson, 2006), bio-optical models (Dall'Olmo & Gitelson, 2005) and self-learning algorithms (Doerffer & Schiller, 2007). Scientists have also attempted to remotely sense sea surface

temperature data and use it as a proxy to monitor algae that show affinity to specific temperature range in the coastal waters of tropical regions (Jutla, Akanda & Islam, 2010).

The challenge: Optical imagery often suffers from the blocking effects of water vapour in the atmosphere. Frequent cloud cover over a region leads to loss of data. This interrupts consistent and complete spatial monitoring of the lakes. Clouds also interfere with thermal remote sensing. On an average, a bloom has a lifetime of several weeks. The short life span of algae further increases the cost of loss of data. For a coastal country like the Netherlands, the issue of data gaps caused by cloudiness and low frequency of satellite overpasses can become a great hurdle in monitoring blooms in inland water bodies. These challenges has propelled the scientific community in the field of remote sensing to look for alternative sensing technology, which is unhindered by clouds (ESA IAP, CyMoNs, 2015).

Microwave remote sensing, a prospect: The active microwave sensor, called radar, is able to sense the Earth's surface irrespective of the cloud cover as microwave radiation penetrates through the clouds (Woodhouse, 2006). Radar measures the amount of reflected/emitted backscatter towards the angle of observation. The signal is sensitive to changes in the physical and electro-magnetic properties of the surface. The algae cause visible change in water surface structure. Poor spatial resolution of radar images had been deterring scientists to explore applications of radar imagery for example in algae monitoring (Cutrona et al., 1961). Development of radar system od sensors, called Synthetic Aperture Radar (SAR) in late twentieth century marked improvement in the spatial and temporal scale of radar images (Cutrona, 1990). The latest progress (especially the launch of Sentinel missions) in the field of space radiometry has led to a remarkable increase in SAR data density from both improved spatial resolution and frequent revisit time (Torres et al., 2012). The SAR application for algae detection was originally found from the errors made by oil spill detection algorithms. It was found that sometimes algal blooms in seas, oceans and lagoons are visible in SAR images as dampened region (Brekke & Solberg, 2005). These blooms caused a similar dampening effect in SAR image as oil spills do. Bresciani et al. (2014) presented an approach of combining SAR and optical data for monitoring algal blooms in the

Curonion Lagoon. The focus of the current study is to explore visibility of algae infestation in SAR images of two lakes smaller than the sites that had been used to monitor algae in existing literature. Images from satellite Sentinel-1a are used. The satellite was launched in April 2014 and has the high pixel resolution of 10 m and revisit time of 12 days. The revisit time has further reduced to 6 days after the launch of Sentinel-1b in 2015.

Current interest: The developments in radar remote sensing and the rising issue of algal blooms in Dutch lakes has received attention from research community. This research has been performed in association with Water Insight, a Dutch company who specialize in analyzing water quality of lakes using remote sensing and in-situ data. Their work in the Netherlands includes data analysis for lake Paterswoldsemeer, one the two study sites of this research. They have offered data for validation and other knowledge support related to lakes in general and lake Paterswoldsemeer in particular for this research.

Scope: This study is exploratory in nature and aims to discuss the visibility of algal blooms in lakes using Sentinel 1 C-SAR images. In this study, I have interpreted C-SAR images of two lakes, lake Utah and lake Paterswoldsemeer with varying conditions and located in two continents. I have built a systematic understanding of processes that are visible on the surface of a lake in C-SAR images. The motive is to detect changes in these processes in the presence of algal blooms that may lead to visibility of booms in C-SAR images. To perform the analysis, a mix of qualitative and quantitative methods is adopted depending on the type of data available for the study sites.

1. 2 Problem statement

Optical images are currently the most common method of sensing and monitoring algae but their use is limited by frequent cloud cover. Radar remote sensing is able to observe the Earth surface through clouds. However, there are not many studies on the detection of blooms using radar images for lakes. Most existing studies on monitoring algae using radar are performed for seas and oceans and not for smaller water bodies such as lakes.

1. 3 Scientific gap and relevance

In the context of rising alarm of toxic algae outbreaks across the world, monitoring of algae in lakes has become of interest to scientists. Radar imaging has been used to monitor wave fields, oil slicks and ship tracking in seas and oceans. Monitoring algal phenology in oceans is the recent application of radar imaging. In this research, I will test if radar imaging can also be applied for smaller water bodies such as lakes. If successful it can contribute to the timely detection of potentially toxic algal blooms in lakes, ponds and reservoirs.

1. 4 Research objective and research questions

The main objective of the study is to explore the use of Sentinel-1 C-band SAR (C-SAR) data for detecting algal blooms in lakes. To achieve the objective, the following research questions will be explored:

I.   What are the factors that cause change in the C-SAR signal from a lake's water surface?

II. Which of these factors support the visibility and detection of algae in a C-SAR image?

1. 5 Outline of the report

This report is divided into five major chapters. Chapter 1 introduces the subject to the readers, it builds a background for the need of this research and defines the research objective and research questions. In chapter 2, the existing knowledge on SAR within the context of this study is discussed. The chapter provides the review of literature referred in the study. Chapter 3 presents the data, study sites and methods that has been used for the study. The Chapter 4 presents the results of the study. Chapter 5 discusses the study results and presents the way forward. Finally, the conclusion of research is summarized in Chapter 6. Appendix sections of the report contain auxiliary data used in this work that may be of interest to some readers.

Chapter 2: Literature study

In this chapter, I discuss some existing knowledge on the subjects of the study. The first section describes key concepts of microwave imaging and the sensing of water surfaces using radar. The literature on radar remote sensing of water surfaces is dominated by the studies on oceans and seas while lakes were ignored because of low spatial resolution. Therefore, to understand radar images of lakes, I describe literature on shallow lakes, which are becoming the target of toxic algal blooms. In the third section, I elaborate on the existing understanding of algae growth dynamics. Finally, the available literature on SAR sensing of water surfaces and its use for monitoring algal blooms in oceans, lagoons and lakes is discussed.

2. 1 Microwave remote sensing

Microwave remote sensing is the measuring of microwave energy that is reflected or radiated by the Earth's surface using a remote active or passive sensor. This process has three key components: i) microwave sensor and scene interaction; ii) sensor design and measurement technique; iii) the application of microwave remote sensing (Woodhouse, 2006). In this study, I have focused on the first and last component of the microwave remote sensing process.

Microwave sensor and scene interaction: There are two kinds of microwave sensors, active and passive sensors. Passive sensors (radiometers) measure intensity of energy emitted by the Earth's surface. This is related to the physical temperature of the emitting layer and the emissivity of the surface. Active sensors, on the other hand, transmit an electromagnetic pulse (of a certain wavelength) and measure the energy scattered back from the Earth's surface. Both types of sensors obey the same physical laws of remote sensing guided by Kirchhoff law (Schanda, 2012) but the measured parameters vary, depending on the sensor characteristics (Wagner et al., 2007). RAdio Detection and Ranging (radar) is is an active system of sensors that illuminates a target by sending a beam of pulsating electromagnetic microwaves and measures the echo reflected by the target. The location of the target is estimated by measuring the precise delay in the echo. These pulsating waves are either horizontally or vertically polarized. Waves travelling perpendicular to the earth surface are called

vertically polarized waves and those travelling parallel to the earth surface are horizontally polarized waves. The measured signal is dependent on both target's surface properties and sensor characteristics (Ulaby & Lang, 2015; Woodhouse, 2006). Sensor characteristics such as wavelength, observation angle (look angle), and polarization of the radar system influence the measured backscatter signal (Valenzuela, 1978). It is necessary that the object of interest appears rough in order to produce a sensible backscatter signal towards the sensor. Therefore, roughness of the surface is always relative to the wavelength of the transmitted signal. Operational wavelength of a sensor is indicated by band. Some of the most commonly used bands in radar imaging are X, C, S and L band (Table 1)[1]. The mission of a satellite program informs the object of study, which in turn determines the bands most suited for sensing the object. When an electromagnetic wave falls on a surface, it generates an electric field (dipole) and the shape of the target determines the orientation of the dipole. Targets with similar orientation as wave polarization produce higher scatter than others (Kalmykov & Pustovoytenko, 1976). Depending on the sensor system, the radar could be single, dual or quad polarized. Single polarized sensors transmit and measure a signal in one plane (horizontal or vertical). The dual polarized sensor sends an incident beam in one polarized plane and receives signals in both horizontal and vertical planes, and the quad-polar sensors can send and receive signals in both polarized planes. Besides polarization, the scatter produced from the interaction of waves with the target is dependent on dielectric property, orientation and roughness of the target (Beckmann & Spizzichino, 1963; Shmelev, 1972). Dielectric constant of a target is dependent on the chemical composition of the surface. It determines the strength of the dipole generated at the interacting surface. Orientation of the object is another important factor in understanding the radar backscatter signal as sometimes it may lead to specular reflection resulting in very low signal. Quantitative measurement of the effective scatter of an object is called scattering cross-section. It is calculated for a certain angle of observation and defined as directional cross section (σ, m^2) as: (Woodhouse, 2006)

$$\sigma(\theta) = \frac{\text{Scattered power per unit solid angle into direction}(\theta) \, [W/\Omega]}{\text{The intensity of the original incident plane}/4\pi \, [W/(m^2\Omega)]}$$

<div align="right">Equation 1</div>

---

[1] Microwave remote sensing was primarily used in military and the band name does not have any relation to wavelength. Instead it was named ambiguously in order to mislead the enemy

where θ is the observation angle, W is the power, Ω is the solid angle and 4π in the denominator is used to normalize the plane wave. For an active sensor system, only the scattered energy from the target that arrives back at the radar system at range R is considered. The scattering cross section becomes radar scattering cross section (RCS) as:

$$\sigma = \frac{I_{received}}{I_{incident}} 4\pi R^2$$

<div align="right">Equation 2</div>

where $I_{received}$ is the intensity received from an area, σ is the effective area that intercepts the signal and redirects $I_{incident}$ towards the sensor. RCS does not have any relation with the actual area that interacts with the wave of the target (Woodhouse, 2006). A radar observes the Earth's surface such that the RCS is proportional to the energy scattered by a distributed area (pixel) rather than a discrete object. There is, therefore, a need to normalize this measurement to make it independent of the size of the pixel. The (normalized) backscatter coefficient is termed sigma nought (σ°), which is derived by dividing RCS by the actual geometrical area on the ground surface and is used interchangeably with terms: *differential radar cross section* or *normalized radar cross section* (NRCS). The most common unit of the radar backscatter value (NRCS) is decibels (db), which is the logarithm of NRCS. Synthetic Aperture Radar (SAR), the radar system of sensor mounted on most radar based satellites currently in space, is a side-looking radar system. It utilizes the flight path of the platform to simulate an extremely large antenna (aperture) electronically, and this generates high-resolution remote sensing imagery. The main source of the data used in this study is data from Sentinel-1 satellite, which is acquired by a C-band SAR (C-SAR) sensor. It is a right-looking antenna with an incidence angle between 20° and 46°. In order to remove the effect of sensor design all SAR imagery undergo a standard set of processing steps and more can be found in (Carrara, Goodman & Majewski, 1995).

Table 1 Currently active radar based satellite missions (Ulaby & Lang, 2015)

Instrument	Wavelength (cm); band	Launch	Description and Use examples	Agency
SMAP radar	23; L-band	January 2015	Makes global measurements of land surface soil moisture and freeze/ thaw state; combined with radiometer (1.4 GHz) measurements.	NASA
ALOS-2 PALSAR-2	23; L-band	May 2014	Using L-band synthetic aperture radar, observes forests and land deformation.	JAXA

HJ-1 SAR-S	9.6; S-band	December 2012	Using S-band synthetic aperture radar, detects environment change, climate change observation, soil moisture retrieval, water cycle monitoring.	CAST
Sentinel-1	6.4; C-band	May 2013	Using advanced C-band synthetic aperture radar to provide all-weather, day- and-night images of Earth's surface; used to monitor ice loss from ice caps and ice sheets and used to map ground movements related to earthquakes.	ESA
RISAT-1	3.5; C-band	April 2012	Using C-band SAR to make all-weather as well as day-and-night SAR observation capability in applications such as agriculture, forestry, soil moisture, geology, sea ice, coastal monitoring, object identification, and flood monitoring.	ISRO
Metop A,B,C ASCAT	3.5; C-band	October 2006	Makes C-band scatterometer measurements of wind speed and direction over the oceans; provide data for ice and land applications, such as sea ice extent, permafrost boundary, desertification.	ESA/EUMETSAT
TerraSAR	2.5; X-band	June 2007	X-band synthetic aperture radar observation of Earth's surface; for instance, observing vegetation for accurate and up-to-date information about the distribution and composition of, and changes in, types of vegetation forming the basis for many applications; utilizing high spatial resolution.	DLR
COSMO SkyMed	2.5; X-band	June 2007	Constellation of four satellites for X-band SAR observation of Earth's surface; applications to environment disaster monitoring, observations of oceans and sea coasts, agricultural and forest areas, radar imaging for cartography.	ASI

2. 2 Water in radar image

Water has a high dielectric constant, thus the scattering by a water surface is very high and is dominated by surface scattering (Valenzuela, 1978). Dielectric constant is a function of incident wavelength, water temperature and its electrical conductivity. Figure 1 shows the change in the permittivity (blue) and the dielectric loss (red) factor of pure water at 0°C (a) and at 20°C (b) as a function of wavelength[2]. The highlighted wavelengths are 3.4 cm (8.9 GHz, close to C-band) and 1.8 cm (16.7 GHz, close to L-band) (Saxton & Lane, 1952). Radar imaging of water thus allows estimation of water temperature, surface composition and structure (Fung & Chart, 1969; Shmelev, 1972). The relation between dielectric constant and backscatter allows to view the phenomenon of wave breaking and swirls in a radar image. Air enters the water column when surface waves are broken. The water bubbles or foam or swirls (mixture of water and air) that appear on the surface has lower dielectric

---

[2] Wavelength can be expressed as frequency as $v = c/\lambda$, where c is the speed of light and λ is wavelength

constant than water (Hwang, 2012). Despite high dielectric constant, the water surface is prone to specular scattering when a water surface is not rough enough compared to the incident wavelength, most incident energy is reflected (and not scattered) in direction opposite to the sensor. This results in a very low backscatter (Barrick & Peake, 1968). A higher backscatter is received from a wavy (rough) water surface. Radar backscatter of open water surfaces is dominated by the so-called Bragg scattering phenomenon (Valenzuela, 1978). The Bragg waves are small capillary waves of a size ranging from mm to cm scale on the surface. These are caused by the shear stress of the local wind field on the water's surface (De Carolis, Parmiggiani & Arabini, 2004). With radar, roughness of the water surface has often been detected up to cm-scale using the Bragg scattering (Woodhouse, 2006; Lehner & Rosenthal, 1998). The close correlation between water backscatter and wind speed is seen for wind field of moderate speed (Attema, 1991). For wavelengths of cm-scale (including C-band) the backscatter of water is dependent on polarization and observation angle of the sensor. The return from the vertically polarized beam at the incidence angle ranging between 20° and 26° is higher than the horizontal return (Wright, 1966; Valenzuela, 1978).
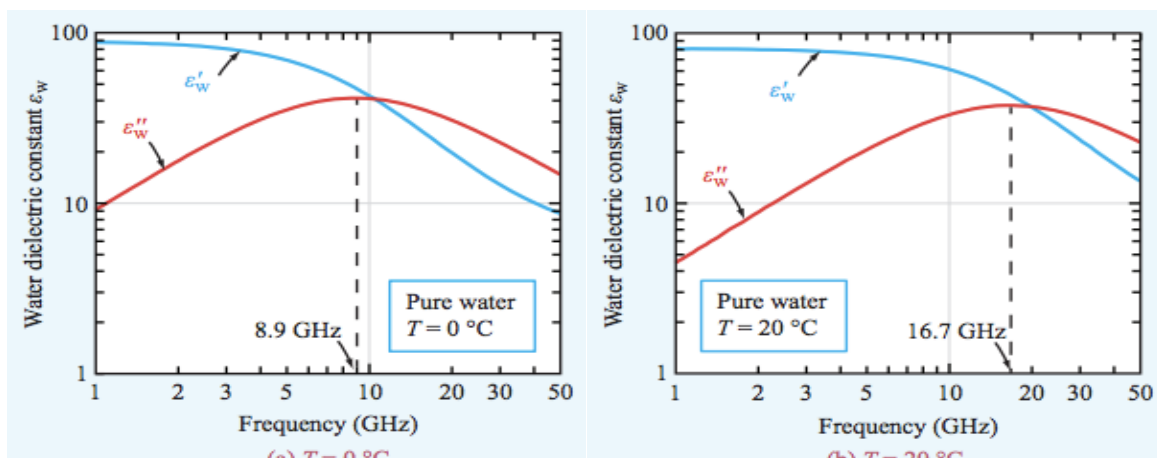
Figure 1 Microwave spectra of the permittivity (blue) and dielectric loss (red) factor of pure water at (a) 0 ◦C and (b) 20 ◦C

(Saxton & Lane, 1952)

Application of microwave remote sensing: Understanding of water properties that are sensible in microwave remote sensing has led to radar applications in estimating wave height, wave spectrum, wind speed, surface currents, and apparent ocean temperature (Valenzuela, 1978). Inverse modelling of changes in these parameters provides insight to the state of a water body at the time of

imaging (Valenzuela, 1978). For example, wind speed retrieval is used in weather forecasting. The algorithm is based on the correlation of water backscatter to the wind speed and has been used to create a wind field map using radar images known as the CMOD4 or wind scatterometer model (Hasselmann, 1972; De Carolis, Parmiggiani & Arabini, 2004). Several versions of the CMOD algorithm exist but these fail (by underestimating the wind speed) on the occasion of high wind speeds (Voronovich & Zavorotny, 2001). Inverse modelling has only been applied on the radar images of an open water surface of seas and the ocean, and the phenomenon that these entail (Shi et al., 2012). An another important application of radar imaging of a water surface, which first brought evidence on the capability of radar in sensing an algal bloom, is detection of oil spills in seas and the ocean (Bern et al., 1992). The presence of a floating layer of oil on a water surface attenuates the Bragg scatter. Basically, changes in the surface composition (which alters the reflection properties) of water cause attenuation in the backscatter signal (Solberg, 2004). The algorithms developed to detect oil spill produced false alarms from algal blooms in ocean and sea. Both oil films and algal blooms caused dampening of the order ranging about 1db to about 12db and were initially difficult to distinguish form each other (Hovland & Digranes, 1994). Later, the difference between the viscosity of the two films helped in discriminating the one from the other. Highly viscous oil stayed together while natural films (algal blooms) were much less cohesive. More recently radar images are being explored to understand algal phenology across oceans (Racault et al., 2012). This has become a leading initiative in understanding ocean's systems and is primarily based on integration of optical and radar images. Analysis of the scatter from a water body using basic radar principles would provide insight on the state of a water surface, research has shown that these interpretations are best when interpreted in the light of hydrodynamics of the water body (Hasselmann, 1972; Phillips, 1966). Radar imaging of the water surface has dominated the field of oceanography. Although most initial research in radar sensing of water bodies was conducted in laboratory tanks and later adopted for oceans, not much study has been done on inland water bodies. The inland water bodies such as lakes have not only different physical characteristics, but they also differ in their chemical and biological characteristics and are highly influenced by anthropological actions (Anderson, Glibert & Burkholder, 2002).

2. 3 Shallow lakes

Surface structure is key to understand the backscatter signal from the surface of a lake, which is intertwined with lake hydrodynamics. Interrelation between water temperature, salinity, water flow velocity, sediments, dissolved oxygen, algae and nutrient concentrations are crucial for understanding the hydrodynamics of surface water bodies (Ji, 2008). The dynamic water density indirectly relates the oxygen and nutrient content. These two properties of water also influence the algae growth. Water has the highest density at 4 °C and the density falls as the temperature of a water body increases or decreases. The change in density of water is not linearly related to the change in the temperature but non-linearly. "The density difference between 20 and 21 °C is approximately equal to the density difference between 5 and 10 °C" (Ji, 2008).

Oxygen enters the water through exchange with the atmosphere and during photosynthesis performed by submerged vegetation in water (Scheffer, 2004). Nutrients enter the water from various sources. However, oxygen and nutrients are distributed mainly by the circulation of the water column (Ji, 2008). During the summer season, the upper surface of the water becomes warmer than the bottom layer. The colder and denser water forms an imaginary layer called thermocline in the water column which prevents mixing between the two layers. Bacteria at the bottom of a lake are always releasing nutrients by breaking down dead vegetation and plants are producing oxygen during the day (Scheffer, 2004). The bottom layer therefore becomes more enriched than the surface layer. During the fall, however, the temperature begins to fall and the difference in temperature between the two layers decreases. This reinforces the mixing of the layers and therefore of nutrients and gases throughout the lake (Ji, 2008).

During summers for shallow lakes, an occasional high wind stress can suspend sediments from the bottom of the lake and break the thermocline. The event transports sediments to the deeper sites and occasionally re-suspends the dormant algae cells to the surface. The turbidity curtails growth of submerged vegetation by decreasing underwater light levels (Ji, 2008). When the vegetation becomes scarce the zoo-plankton (that feeds on algae) becomes an easy target for smaller fish, which plummets their number to an extent that leads to algal blooms. High nutrients and low competition from submerged vegetation can

cause an algal bloom to occur at a rapid rate. This chain of events triggers the seasonal eutrophication cycle of lakes. Eutrophication is a natural process in which nutrients like nitrogen and phosphorous build up in a lake or pond over time (Greeson, 1969).

Therefore, shallow lakes or ponds naturally have two major states of being (Scheffer, 2004). A crystal clear view of the submerged water life, the column and surface showcasing the glimpse of thriving water life is one of the two states of being. In the second state of being, the lake is murky with suspended sediment particles and blooming algae veiling all life. The two states are gravely contrasting but are governed by naturally stabilizing feedback mechanisms of the lake. Intermediate situations between the two are relatively rare (Scheffer, 2004). This natural response of a lake to the environment is being affected by external factors. Human activities in the surroundings are disturbing the balance between the two states by accumulating nutrients in the lake (Ji, 2008). The nutrients leach from the nearby agricultural land, gardens, waste treatment plants etc. More than often the response of shallow lakes to eutrophication has been dramatic (Álvarez et al., 2008; Sellner, 2003). Overloading of nutrients and the inherent advantage of some toxic algae species is causing the algal bloom to grow beyond commonly experienced concentrations. The blooms are lasting longer and accumulating not only in the water column but also on the surface for much longer time frames. The lake dynamics is becoming more unpredictable and vicious (Sellner, 2003; Heisler, 2008; Anderson, Glibert, & Burkholder, 2002; Álvarez et al., 2008). More recently, more harmful blooms have surfaced in water bodies where those blooms were not found inherently. In some of the extreme cases, there has been significant loss of life resulting into a death of the lake (Appendix 1).

2. 4 Subject of study: Algae

Algae are simple aquatic organisms capable of photosynthesis. They exist in a variety of forms, from single celled organisms to large seaweeds. The single celled algae are known as phytoplankton. Algae float along the water current, up-taking nutrients and accessing light for photosynthesis. They are the primary energy producers of water life and lay at the bottom of the food chain. Protozoa and zoo-plankton feed on phytoplankton, which are in turn grazed by small fish and so on. Despite their crucial role in lakes and marine ecology some plankton

species are great nuisance and are capable of disrupting the ecological and nutrient balance of shallow lakes (Wetzel, 1983; Hansson, 1988). One such algae type is blue-green algae.[3] A rapid increase in algae population occurs when there is increase in the concentration of nutrients in a lake accompanied by favorable light and temperature conditions. This leads to phenomena called "algal blooms" (Medrano, 2014). Presently filamentous green algae and blue green algae bloom; the two key subjects of this study have become a great matter of concern to the management bodies of lakes across the world.

Filamentous green algae develop into thick slimy surface films, which interfere with boat passages, recreational activities and general aesthetics of the surroundings. Although a green algal bloom is an unpleasant sight, it is not harmful. The nature of blue-green algae, on the other hand, is much more notorious. Under favorable conditions, it multiplies at accelerated rates and forms scums, a visible floating layer on the surface. Their cell is surrounded by a gelatinous sheath which allows them to grow into dense colonies. Occasionally scums can be inches in thickness. Scums bring high concentrations of blue-green algae containing hazardous concentrations of potent toxin to the water surface (Medrano, 2014). At the occurrence of such an event, water managers issue health warnings in media and at all the access points of the lake (Meriluoto & Codd, 2005). Exposure to toxic scums pose a direct threat to human and animal health (Chorus & Bartram, 1999). Further, the decomposition of blooms causes oxygen depletion in the water body and may even cause death of fish-stock. Besides, the decomposition of blue-green algae is a sensory stimulating process that generates pink, blue or white pigments giving a variety of colors to the scum and produces an awful bad odor (GLaSS D. 5.7, 2015).

The meteorology, hydro-dynamics and biological and adaptive characteristics of an algae species are the main factors to the determination of the spatial distribution of concentrations of the bloom (Medrano, 2014). The lake turbulence and hydrodynamics influence the availability of nutrients and the light environment, which directly impact algae growth and movements. A

---

[3] It is one celled algae, thus a phytoplankton, and also qualifies as bacteria, which is why it is also known as cyanobacteria. The scientific community is battling about categorization of cyanobacteria as algae. For the purpose of this study, however, cyanobacteria are addressed by its popular name which classifies it as algae, the blue-green algae.

turbulent lake may support some algae species while dwindling other species (Medrano, 2014). For example, some blue-green algae are buoyant and have evolved to control their buoyancy. This allows them to migrate vertically within the water column to optimize the light and nutrients distribution (conditions) within the lake and multiply in colonies. In a turbulent lake, however, the blue green algae may lose the advantage of being buoyant when the current brings other species such as green algae to the surface (Medrano, 2014). As a result, algal blooms follow a complex temporal and spatial dynamics (Sellner, 2003). This makes monitoring a daunting and costly exercise using conventional water-sampling methods (Liu, Islam & Gao., 2003).

2. 5 Sensing algae infested lakes

Algal bloom is a common phenomenon in a eutrophic lake when the light conditions become optimal (Ji, 2008). It is found that algae produce hydrocarbon products bearing properties similar to oil (Han et al., 1968). This property provides the gateway to transfer available knowledge on radar sensing of oil to algae. For most algae species it is, however, not known when and how this oil like product appears on the surface as surfactants (Medrano, 2014).

Blue-green algae is different from most algae as this species can undergo many transformations and are genetically more dominant and adopting to the surroundings. Inherently, the blue-green algal bloom follows a deterministic motion in the upper layer (first 4 m) of the water column, which is usually the mean depth of the inland water bodies (Visser, Passarge & Mur, 1997)[4]. The size of the colony has effect on the depth to which the algal bloom might migrate in the water column, which is now believed to be the reason behind a sudden appearance of the bloom (O'Brien, Miadlikowska & Lutzoni, 2005). When an algal bloom becomes sufficiently large, it is able to move within the water column together as a unit and show immediate response to changes in the environment (relating to nutrients, light or other conditions) (Kong, Ma, Gao & Wu, 2009). A medium sized colony concentrates in the middle of the top layer, whereas a larger bloom is able to migrate to greater depth and may only need to surface occasionally. Strong wind shear stress may entrain a colony

---

[4] With time and exposure to light, the particles produce more carbohydrates, which increases their density. Eventually their weight makes them sink, where the light conditions start to diminish. Thus, the carbohydrate stocks begin to decline and they become lighter again that allows them to move to the surface again.

redistributing the individual cells of algae in the lake (Medrano, 2014). It is found that when the concentration of algae becomes high enough to saturate surface layers with oxygen gas, the gas forms bubbles. It is easier for the bubbles to escape from a turbulent water body. However, in the absence of turbulence with only mild wind condition, oxygen gas bubbles grow inside or become attached to the mucilage (the gelatinous sheath) present in the cell wall of blue-green algae. This brings the algae colonies to the surface having an irreversible buoyancy effect to form scums.

Bresciani et al. (2014) studied the Curonian lagoon at the Baltic Sea and applied a combination of data including C-band SAR imagery to sense blue-green algae infestation. They performed an empirical analysis by correlating the chlorophyll levels derived from optical imagery with the attenuation in SAR backscatter. They found that a higher concentration of algae caused greater attenuation in SAR imagery under moderate wind conditions (Bresciani, et al., 2014). It was also shown that the attenuation was related to the species of blue-green algae. The Curonian lagoon is a large size water body (area of the order of 1000 km^2) in comparison to an average lake size (usually of the order of 100 km^2). Secondly, the lagoon suffered from intense algal blooms, the concentration of blue-green algae increased upto 500 milligram per cubic meter. Such high intensity is rare in the lakes as often in case of an intense bloom, the water management authorities had to intervene. Another study has been performed for Lake Taihu in China to sense algae in C-band SAR images. The study used machine learning algorithms to classify dark regions in SAR imagery as regions suffering from algae and validated it with optical imagery (Wang et al., 2015). It was found that dark regions of area of the order of 10 km^2 were better classified than those of the order of 100 km^2. The size of lake Taihu is twice the size of the Curonian lagoon. Both studies used optical imagery for training and validation. The studies clearly provide evidence of the potential of SAR imaging for sensing algae in lakes and semi-enclosed water bodies such as lagoons. However, the massive size of the study sites in both cases is beyond an average size of a lake. The need for optical imagery in the two research papers stretched the time scale of these studies to years as it is very rare to find good quality optical imagery that is acquired on the same day within reasonable time difference (of a few hours) as the acquisition of SAR imagery. Also, none of the two studies discuss the factors affecting the SAR signals that would enhance the understanding of SAR images for sensing algal blooms. The nature and

causality of correlation between indices for algae, derived from optical imagery and the attenuation in VV backscatter signal is not fully understood. There is no study that explains changes in water surface backscatter signal from a view point of lake hydrodynamics and algal growth cycle. In this research, I have attempted to build understanding of radar remote sensing in light of its two subjects of study: lakes and algae. The current study is aimed to find if the results found by the two mentioned studies can be applied to lakes of much smaller size and with varying density of algae. In this study, I have validated SAR data primarily with in-situ data instead of completely relying on optical imagery.

Chapter 3: Methods

In the previous chapter, I have discussed literature that presented the potential of C-band SAR imaging in sensing algae (Section 2.2 and 2.5, Chapter 2). However, there exists very little understanding on the interpretation of C-SAR images for lakes in general. Radar remote sensing for water has primarily been dominated by studies on oceans and seas (Section 2.2). Knowledge of radar remote sensing for oceans cannot be directly applied for lakes. The forces at play in a lake are significantly different from that of oceans and seas where forces act more on global scale than on local scale. The focus of this research is to build systematic understanding on factors that guide the visibility and detection of algae in lakes, which are ever so changing. Methods employed for the research are mostly exploratory and are described below:

1. *Selection of the study sites.* A lake unfamiliar to the author, lake Utah, was studied to build a hypothesis about factors that affect water backscatter in lakes. The lake was selected because it was suffering from an intense algal bloom during the start of this research, June 2016 (Appendix 1a). There was no data available on the exact timing of occurrence and spatial distribution of the bloom. The only guiding information was discrete maps of the concentration of algae in water samples collected at given locations by the water authorities of the lake. Besides lake Utah, a relatively familiar site, lake Paterswoldsemeer in the Netherlands, was studied to test the formulated hypothesizes. The lake also suffered from algal blooms. Although the size of the lake and blooms was smaller than seen in case Utah, more information was available on the spatial and temporal spread of bloom for the lake.

2. *Preparation of data:* Data was gathered from different sources and was processed for analysis for both sites.

3. *Qualitative analysis of data on lake Utah:* The Utah site was studied qualitatively to locate factors that allow visibility of algae infested regions of the lake.

   a. Following the evidence in literature on importance of wind stress for visibility of the water surface in radar imageries, first, water backscatter for each image was related to the wind speed.

   b. Next, dampened regions in the imagery were related to the wind direction. Direction of wind causes different physical objects to act as wind shields causing the wind shield effect.

c. Each imagery was assessed in view of both wind conditions and local effects of the shields to locate algae infested regions. The interpretations were then used to develop a hypothesis to be tested using data for the study site of the Netherlands.

4. *Quantitative analysis of data on lake Paterswoldsemeer:* Hypotheses formulated from the lake Utah study were tested for Paterswoldsemeer. Following this, spatial and temporal differences in the backscatter within and across the lake were analyzed. Finally, the conditions that make algae visible are highlighted and summarized in the results.

In the sections below first the study sites for the research are described. Then data sources and data processing for all data included in the study are discussed. Finally, the last two sections discuss methods adopted for qualitative and quantitative analysis of the two study sites.

3. 1 Study Sites

Lake Utah lies in state Utah of the United States of America and has been used to develop a hypothesis on factors that guide visibility of algal blooms in radar images of lakes (Fig. 2). Utah Lake is a shallow (~3.2 m deep on average) freshwater lake and spreads across 370 km^2 of surface area. It lies in Utah Valley, surrounded by two mountain ranges along the south-eastern and north-western shore and the Provo-Orem metropolitan area along the north eastern coastline. The lake's only river outlet, the Jordan River, is a tributary of the Great Salt Lake (Fig. 2). Evaporation accounts for 42% of the outflow of the lake, which leaves the lake slightly saline. The elevation of the lake is at 1368 m above sea level. When the water level increases, the pumps and gates on the Jordan River are left open. The lake contains a small island called Bird Island, about 3.62 km north of the Lincoln Beach around the middle of the lake. The island has a few trees and is somewhat visible from Lincoln Beach. The island may completely submerge when the water level rises and the trees become the only indication of the island being there. Due to its proximity to the Provo-Orem metropolitan area, Utah Lake is a fairly popular recreation destination. In the summer, fishing, water skiing, boating, camping, and picnicking are the most popular activities. During the winter, ice fishing, ice hockey and ice

skating are popular on the lake especially at Utah Lake State Park and Lincoln Beach (US Government, 2016).

Utah lake is known to suffer from plankton blooms. The algal bloom for year 2016 was the worst in the last thirty years (Fig. 3, Appendix 1a). The concentration of harmful algal blooms for the time period between May and September 2016 was well-above safety levels. Besides, the geography surrounding the lake make the lake an ideal site to study local effects of wind shields (or the wind directions) in radar images. Additionally, the size of the lake allowed for the development of surface patterns from wind shear stress. Interference of waves from the wind-stress and waves driven by lake hydraulics (often related to lake bathymetry, inflows and outflows) had greater likelihood to be captured in radar imagery than in the case for a small lake. The influence on the developed wave patterns on the lake from the presence of the only physical structure in the lake, the Bird Island, was ignored due to its small size.

SAR data has inherent speckle noise and the interpretation of the imagery is often very challenging. Water surface can be disturbed by a numerous reasons, which get reflected in the data. The element of unfamiliarity of the lake made it easier to overlook effects in radar imageries, which were not related to the subject of study and thus was apt for developing hypotheses.

Figure 2 Lake Utah with an overlay of bathymetry.
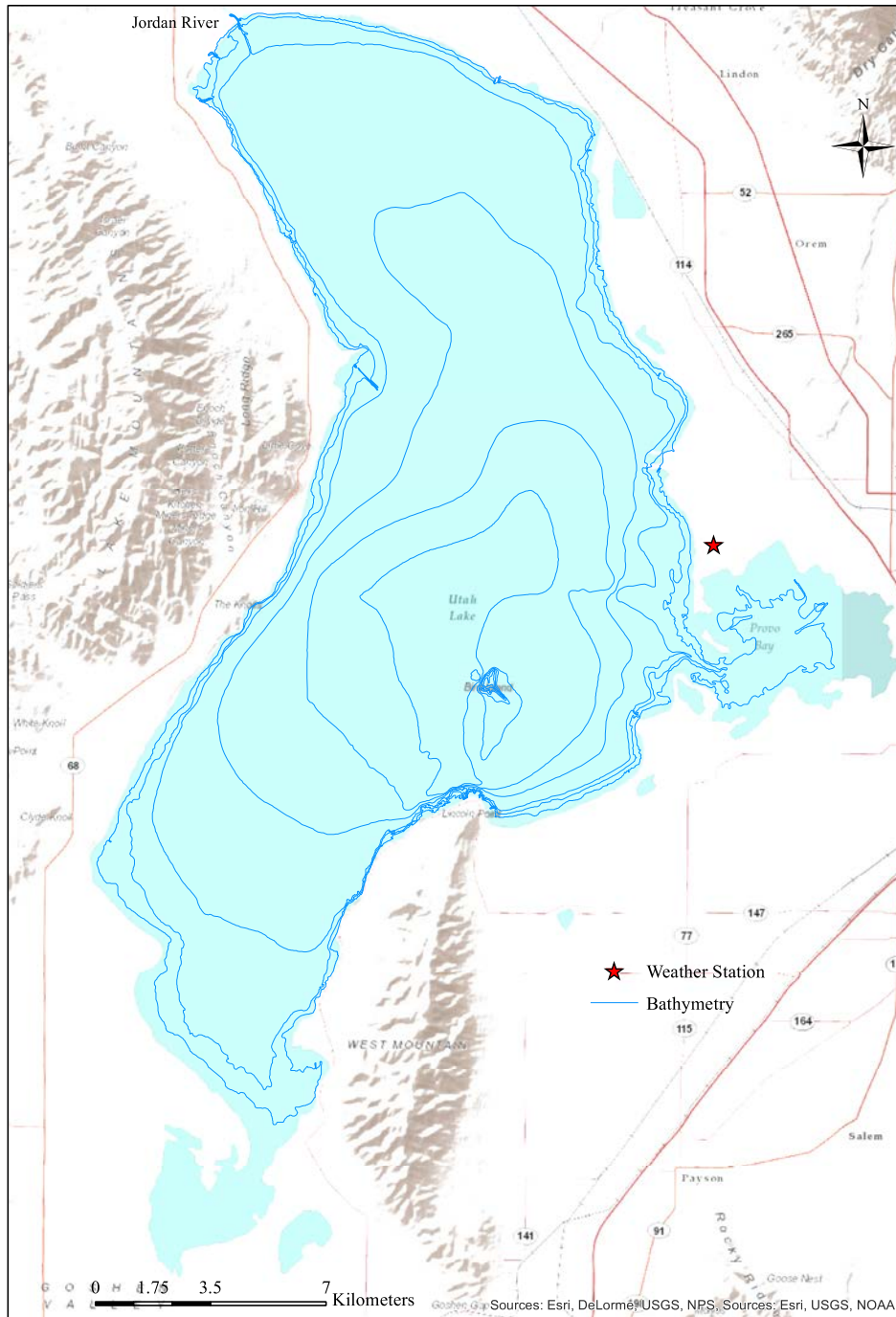
Toxic algae bloom closes Utah lake, sickens more than 100 people

July 14, 2016: This photo shows discolored water caused by an algae bloom near the Lindon Marina in Utah Lake in Lindon, Utah. (Rick Egan/The Salt Lake Tribune via AP,)
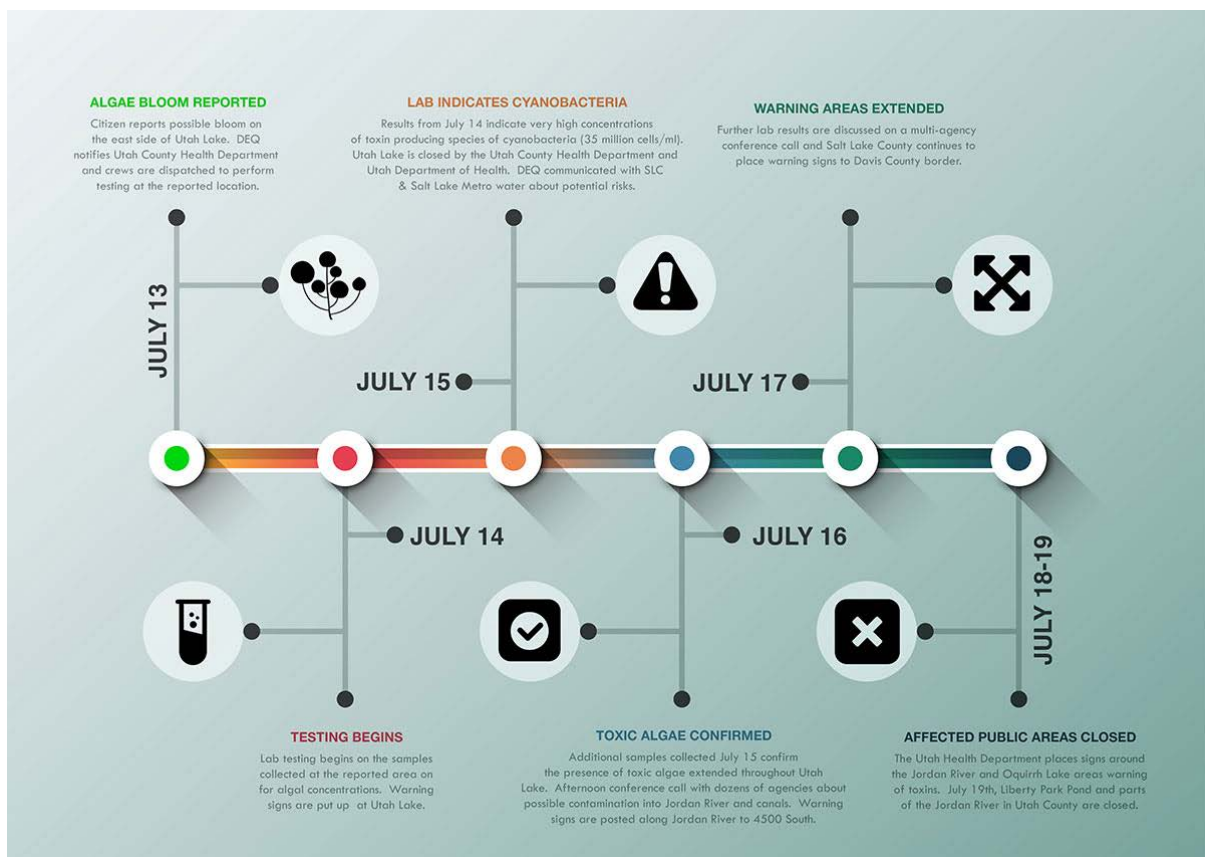

Figure 3 Utah Lake algae blooms in the news (top) with the schema of events/actions of water authority from the month of July (bottom)

Lake Paterswoldsemeer, the other study site, is located in the Netherlands. It is a relatively small lake. It is 1.7 km^2 in surface area (Fig. 4 and Fig. 5). Lake Paterswoldsemeer is located on the south side of the city of Groningen, which is located in the North part of the Netherlands. Peat mining at the site led to the creation of this lake. Therefore, it is not deep (the maximum depth ~ 3 m) and it has several small bays and islands along the shorelines. The lake is a popular spot for recreation, especially for swimming, surfing and boating. The lake often suffers from algal blooms and, therefore, a dike was built to fence off the area around the beach. The Paterswoldsemeer water management system consists of a complex chain of channels and locks. The water is fed from lake IJsselmeer, wherefrom it leads northwards via lake Paterswoldsemeer into the Wadden Sea. The management requires many manual decisions about closing and opening of locks to maintain the water level, especially for inland commercial shipping (in the channel of water bodies feeding and discharging the lake) that needs stable water levels: deep enough for the larger boats, low enough for the same boats to pass under the bridges. Noorderzijlvest is the local water authority responsible for the general water level and water quality regulation of the lake.

Regularly Paterswoldsemeer also suffers from intense blooms of potentially toxic blue-green algae and therefore has attracted interest of ecological and socio-economic stakeholders. The site is being used as test location for algae detection by remote sensing and it is one of the use cases of the ESA project called CyMoNs (ESA IAP, CyMoNs, 2015). At the occurrence of scums, the bathing area is closed down, which causes losses for the local entrepreneurs in the recreational industry. The potential toxic threat has caused decline in the recreational economy of the lake. It has been observed that occasionally scums enter the lake via the inlet lock, but in other cases the source of blooms is harder to locate. Monitoring is expected to increase the knowledge on the appearance of blooms and contribute to water quality management (GLaSS D. 5.7, 2015).

Figure 4 Cyanobacteria bloom in lake Paterswoldsemeer (left), bathing in lake Paterswoldsemeer (right). Photos: Water Insight partner, BlueLeg Monitor
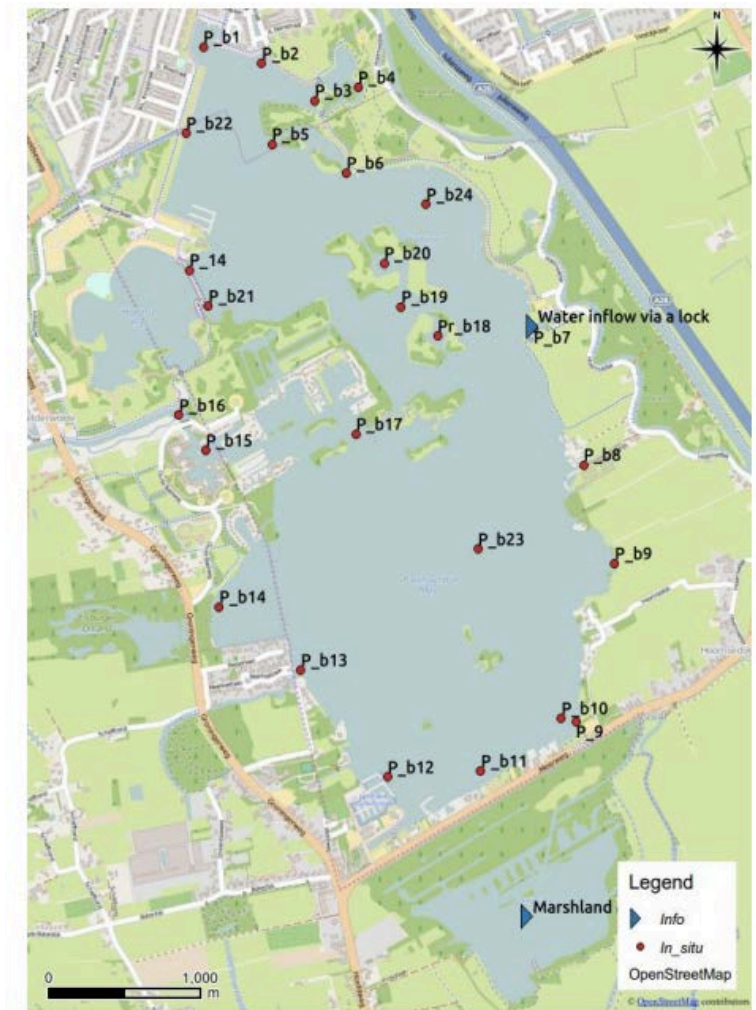

Figure 5 Spatial distribution of in-situ measurements (WISP stations) for lake Paterswoldsemeer (ESA IAP, CyMoNs, 2015).

3. 2 Data

Source:

1. Sentinel-1 C-Band SAR Images

The key data for the study was sourced from the free online database (Scientific Sentinel Hub) of the Sentinel-1 satellite, launched under the Sentinel mission of the European Space Agency (ESA) in 2013. Part of the data was downloaded using the manual-interface of the sentinel scientific data hub and the rest from the data hub api via a script made available by Water Insight. The C-SAR sensor mounted on Sentinel-1 is a dual-polarized radar instrument. It is a right-looking, active phased array antenna and performs fast scanning in range (elevation) and azimuth direction. The operational wavelength for the C-band sensor is approximately 5.6 cm. Dual H and dual V (HH+HV, VV+VH) are the two polarizations of the C-SAR instrument. For land, dual V (VV+VH) polarization chains are operated (ESA, 2016). However, single VV-polarization data was used to study the two study sites because this polarization enhances water backscatter and is most suited for radar remote sensing of water (Section 2.2). The Sentinel-1 data products range from level 0 to 2. The level-1 product was used for this study, which is available in two data formats: SLC (Side Look Complex) and GRD (Ground Range Data). For this study the GRD dataset was used, because it is focused, ellipsoid corrected and multi-looked, which saved time by reducing data processing steps. Since the focus of the study was towards application of C-SAR data, more time was spent on analysis than on processing of the data. The details on pre-processing steps that the product underwent at the data center of ESA can be found at https://earth.esa.int/web/sentinel/technical-guides/sentinel-1-sar/products-algorithms/level-1-algorithms/overview. The data for Utah included C-SAR images acquired between March and August 2016. This range was selected because the lake was mostly in the frozen state before March and the algal bloom in the lake lasted until the month of August (Appendix 1a). Also, images beyond August were not included for Utah because of the research schedule that did not allow inclusion of more data during the analysis period for lake Utah. For lake Paterswoldsemeer, C-SAR images for months between January and October 2016 were included. Although the Sentinel-1 temporal resolution is 6 days, not all images were available.

2. Meteorological data

Radar images of a water surface is sensitive to wind shear stress and, therefore, meteorological data was included in the study. For Lake Utah, information about shear stress was approximated using wind data that was collected from

the website: www.wunderground.com. This data was sourced from the Provo-Bay weather station (named: KPVU, Provo mini-airport) and was available at half hourly to hourly basis. Similarly, the meteorological data for lake Paterswoldsemeer was sourced from weather stations at airport Eelde located few kilometers to the south-west of Groningen city and collected from the same website. Since this weather station was relatively farther from the lake, part of the meteorological data was sourced from a weather station mounted on the lake itself. This data was not available for the whole timeline of acquired imagery, but whenever available, was given a preference (Appendix 1b).

3. Chlorophyll distribution maps

The algal bloom distribution maps derived from optical imagery, acquired from the Sentinel-2 and Landsat-8 mission, were received as ready to use products from Water Insight. These maps provided the spatial distribution of the concentration of chlorophyll (in the water column) in the two lakes. The algorithm used to produce the maps is designed to estimate chlorophyll in the water column. But the algorithm is not fit for estimation of chlorophyll concentration on the water surface in the presence of scums. This was used as validation data for the two lakes. Unfortunately, often good quality (cloud-free) optical images were not available for the same day, let alone the same hour, as C-SAR images used in the study.

4. WISP and in-situ data

For lake Paterswoldsemeer, in-situ hyper-spectral data recorded by the Water Insight Spectrometer (WISP-3) at WISP stations (Fig. 4) along with time stamped photographs was available for the month of June and July 2016. Therefore, this data was also used for analyzing C-SAR images of lake Paterswoldsemeer.

5. Algae concentration maps

For lake Utah, distribution maps of algae concentration were available at the lake Utah official website. The map provided information on algae concentrations found in samples collected at the given location by the water authorities of lake Utah during the time when the lake was severely infested with algae. Two such maps were available for days in the month of July and August.

6. Bathymetry data

The bathymetry data (shape file) for lake Utah is downloaded from the US government database on geography. For lake Paterswoldsemeer this data was made available by Water Insight.

7. Interviews

An interview with an expert of the water authority Noorderzijlvest (responsible for lake Paterswoldsemeer) was conducted for his comments on the interpretations made about presence of algae or other artefacts or algae lookalikes in the radar imageries for days when no other data was available. The information about the Dutch site was used to substantiate the analysis and interpretation of radar imageries for lake Paterswoldsemeer.

8. Photographs

Photographs for a few days during the month of June and July are available for the study site lake Paterswoldsemeer. This data is used to visualize the lake surface during the presence of algal blooms.

Tools:

1. SNAP

Besides the open Sentinel data hub, ESA has made available open source toolboxes to analyze EO data. The tool used for processing Sentinel data is called Sentinel Application Platform (SNAP) (ESA website, 2016). The software is easy to use and able to handle most commonly used image formats such as Geotiff, Netcdf, csv, etc., but was constantly under development during the time of study. Despite offering standard processing features, the software presented challenges due to its ever evolving nature and bugs located by the user and developer community. Free access and easy handling of the variety of files are the main reason for choosing this tool to handle radar imageries. Other software capable of handling radar imageries, for example *gamma,* is only available at a cost not affordable for this study.

2. QGIS and R

Following the general processing of the radar imagery, the later analysis was performed using QGIS software and RStudio (the editor for R programming language). These is also open source software (available for free), but more

mature than SNAP. I used the long term support versions, QGIS-4.10 and RStudio 3.2.2 for the study. For the first study site, data was analyzed qualitatively using QGIS. A descriptive analysis was performed and described in the Section 4.1. For the second study site, quantitative methods were adopted. R scripts were created to perform the analysis.

Processing Sentinel-1 C-SAR imagery:
Despite being a level-1 product, the downloaded imageries required some additional processing steps in order to make the image data easy to interpret and comparable in space-time. This involved the following steps:

Reading the data: SNAP reads compressed Sentinel-1 downloads directly. In order to get correct North orientation, the image requires geo-coding. But first, a processing step called 'apply orbit file' is done to read all auxiliary information of the product. This step loads the precise information about the satellite flight path, coordinates, time and direction to the read product as an orbit file contains information about the recording time, coordinates and quality of measurement for every single pixel in the image. This information is necessary for geocoding the product.

Speckle reduction: This was done in two ways: multi-looking was performed for lake Utah and by applying a refined sigma Lee speckle filter for lake Paterswoldsemeer.
A radar image is multi-looked during the pre-processing, because the raw SAR imagery is compressed along the horizontal direction. Therefore, multi-looking is applied to create a nominal image pixel size[5].
For more information please refer to https://earth.esa.int/web/sentinel/technical-guides/sentinel-1-sar/products-algorithms/level-1-algorithms/overview.
However, the multi-looking can also be used to decrease speckle noise (De Vries, 1998). This was performed because it reduced noise and at the same time improved the radiometric resolution. However, for lake Utah the spatial resolution was degraded from 10m to 20m. Degradation of spatial resolution for lake Utah was feasible because of its large size, but was not feasible for lake Paterswoldsemeer. Due to the small size of the lake Paterswoldsemeer, decrease in spatial resolution would mean loss of data from the border of the lake, which

---

[5] Multi-looking reduces speckle by incoherent addition of independent looks obtained by partitioning the signal beam along the range and/or azimuth of the same scene.

is often the most susceptible region to algal blooms. Hence for this lake, a refined Lee filter speckle filter was applied to the imagery. The filter preserves the edges and de-noises the image. In this filter, the de-speckled pixel value is a weighted sum of the observed (central pixel) value and the mean value. The weighting coefficient is a function of local target heterogeneity measured through the coefficient of variation. This filter does not degrade the spatial resolution, but only the radiometric resolution.

Radiometric calibrations: Calibration to sigma naught values (NRCS) is performed on the multi-looked product to enable comparison of SAR imagery acquired on different dates, with different sensors or with the same sensors but different acquisition modes or differently processed. It is a dimensionless number and the values describe the relative strength observed from the target to that expected from an area of one square meter (ESA).

Linear to db: A logarithmic scale is applied to the calibrated values. The generated scale is much more enhanced and it makes interpretation easier.

Geo-coding and topographic normalization: SNAP displays the product in radar geometry called the ground range. Using the SNAP range Doppler terrain correction tool all radar imagery for lake Utah were geocoded using 30m SRTM-DEM into the UTM-12N projection coordinate system and for lake Paterswoldsemeer into RD-New WGS84.

Preparation of processed data for analysis: Clipped to the area of interest; the C-SAR imagery was processed before creating a subset for the region of interest (lake Utah or lake Paterswoldsemeer). Lake Utah was clipped using the shape file of the lake downloaded from the US government database on physical objects of state Utah.

Renaming of all images to include meteorological data: All images were programmatically renamed to include information on wind speed and direction along with the date of image acquisition to make analysis and interpretation of an image easy and hassle free.

Temporal stacking of all imagery: Lake Utah images were easily stacked using a function called stack available in R in raster package. However, it was not the

same for the other site. It was found that images had different dimensions, extents and number of rows and columns. Therefore, for successful temporal stacking of the images, all images were resampled using a function created in R to achieve exactly same number of rows and columns and an extent which was common to all raster.

3. 3 Data analysis

Qualitative analysis of Utah Imageries

For each C-SAR image water backscatter was described in relation to the following:

a. Variation in water backscatter across the lake was assessed in a hierarchical manner as described below:

    i. First, the backscatter is related to the wind conditions on the surface.

    ii. Besides wind speed, the effect of wind direction is analyzed. The lake is surrounded by two stretches of mountains, one on the north-western border of the lake and the other along the south-eastern border of the lake, which cause wind shield effects. A wind shield effect is a change in backscatter signal in a certain region due to the presence of a physical object that causes a local change in the wind stress experienced by a water surface. This leads to local differences within an image.

    iii. If the relation of backscatter is not fully understood by wind conditions, water properties like temperature and past weather record is used to explain the backscatter from the water surface.

    iv. Next, the interconnectivity of the lake with other water channels (inflow or outflow), lake bathymetry and other possible factors are assessed for their effect on backscatter.

    v. Finally, the possibility of algal blooms is considered and validated with the algae concentration maps or optical image of the nearest date.

b. At the end of the analysis of all available imageries for the lake Utah, a set of hypotheses were formed, which then became the guiding factors for the quantitative analysis of the lake Paterswoldsemeer.

Analysis of the lake Paterswoldsemeer

The lake Paterswoldsemeer was analyzed quantitatively to test the hypotheses generated using the data for lake Utah. The analysis was performed along the following steps:

a. A site was selected to represent the average backscatter of the lake. This site was chosen such that it does not suffer from a wind shield effect irrespective of the wind direction and has on average a long fetch. Fetch is the distance along which a wave can develop and travel without any interferences from borders, or any other physical obstructions. For both temporal and spatial analysis, the data from this site was considered as a reference. Any deviation at a site of study from the reference site was interpreted as local effect.

b. Since the radar backscatter is a noisy signal, the backscatter value per pixel is less meaningful information compared to a signal averaged over time or over space. In order to analyze the backscatter signal at a location of available WISP measurements of chlorophyll concentration or presence of blue-green algae scums, or with respect to wind stress received at the location, the backscatter signal at that point is redefined. Windows of different sizes were created around the pixel containing the point. The size of the window was chosen after gradually increasing the window size and observing the signal distribution within the pixel. Once the distribution of the signal from each pixel in the window was stable or reached normality, the window size was fixed and used for redefining all backscatter signals that needed to be analyzed or understood in view of point data observations on chlorophyll concentrations and presence of scums.

c. The mean backscatter signal for all images was calculated for the reference site by averaging backscatter of all pixels contained in the window around the pixel containing the reference point (size was found in the previous step). This value was then plotted against the wind speed to see the relationship between the water backscatter and wind speed for all observation days.

d. All images were divided in two batches, one containing images from the time when the lake suffered from an algal bloom and the second batch contained images for the time when the lake was free from algae. For each batch, the mean backscatter-signal per pixel was calculated. This

produced two mean rasters, namely: "mean backscatter during algae infestation" and "mean backscatter without algae infestation". This step was performed because averaging of images in a batch would i) filter out noise in the backscatter signal, and ii) provide an overall difference during the two states of the lake. Here any impact of weather conditions was ignored.

e. It was possible that an image in one of the two batches may act as an outlier and dominate the mean raster. In order to eliminate this possibility, one image was randomly removed from the batch while calculating the mean raster. This step was repeated a few times to check consistency in the result from the step d.

f. In addition, a temporal analysis was conducted for three WISP stations (Fig. 19). These stations showed a high concentration of algae. The backscatter signal at the WISP stations was averaged for pixels contained in the window found in step b. To understand changes in backscatter as time progressed from March to September, mean backscatter around the WISP station is plotted against time. In the same plot wind speed is also plotted against time.

Chapter 4: Results

This chapter is divided in three sections. The first section discusses the results of study site lake Utah. The following section discusses the results from the study of lake Paterswoldsemeer. In the last section a summary of key results is presented.

4. 1 Utah Lake case study

For lake Utah, processed radar images were analyzed qualitatively. To observe the effect of wind speed without the effect of direction, images with similar wind directions are discussed together. All images are classified in five sets of groups based on the wind direction namely, 1) images acquired with wind direction ranging from South to West, 2) images acquired with wind direction ranging from West to North, 3) image acquired during with wind direction ranging from East to South, 4) images acquired during the changing wind conditions and 5) image acquired during calm weather. No image was acquired at a time when wind blew from the direction between North and East. Perhaps during this time of the year, the lake does not receive winds from North East.

The first group contains images acquired during the time when wind direction, as recorded at Provo bay weather station, was between South and West. Figure 6 shows the image acquired on 30 March 2016. The wind speed at the time of acquisition was about 4.1 m/s, and was blowing from South South-West direction. The overall backscatter in the image is high and there is dampening at Lincoln point. This dampening is due to the wind shield effect (Section 3.1). The West mountain provides obstruction to wind blowing predominantly from South. On closer look, the image shows streaks along the wind direction at the center of the lake. The mean temperature on the day was 4°C.

The wind conditions at the time of acquisition of the image dated 23 April 2016 (Fig. 7) was 7 m/s, blowing from West South-West direction. The image displays high wind stress as dampened and brightened streaks of backscatter signal along the wind direction. The long fetch (open area along the wind direction) between Mosida and Utah State Park has more pronounced streaks. The image also exhibits wind shield effects. The effect is visible along the foot

of Lake mountain (around Pelican Point), where the backscatter is slightly dampened. The backscatter in this region is more homogeneous and does not show streaks along the wind direction. The mean temperature on this day was 19° C.

At the time of acquisition of the 10 June 2016 image (Fig. 8), the direction of wind was South-West West-South-West and the wind speed was 6 m/s. This image also shows high wind stress as streaks along the wind direction and dampening at the foot hill of Lake mountain due to wind shield effect. However, the dampened region is larger, falling between the Jordan River and Pelican point all the way till Lindon Marina. The slight change in the direction (as compared to Fig. 7) has caused the change in wind stress over a larger area. Again the dampened region has lower backscatter and is absent of streaks. The mean temperature on this day has increased considerably to 27°C.

The last image of the first group was acquired on 4 July 2016, at the time, wind was blowing at 11 m/s from South (Fig. 9). The image also shows streaks along the wind direction, however, these are less pronounced in the southern region than the northern region. The effect of the wind shield from the Lake mountain may explain the dampening in a small area around Jordan River and Sartoga Springs. However, wind shield does not provide explanation to dampening along the edge between Utah State Park and Lindon Marina. Among known facts of algal bloom in the Utah case is that on 14 July 2016, the bloom was intense at region between Lincoln Point and Lindon Marina (Fig. 12 & Appendix 1a). Therefore, a possible explanation for this dampening can be the infestation of algal bloom (Fig. 12). However, there is no data from this date for validation.

In all the four images of this group, we see the effect of increase in wind speed and wind shield effect from the two mountains. This group also captures images with different climatic conditions. The temperature increased from 4° C (30 March) to 27°C (14 July, 2016) but the effect of increase in temperature can not be seen directly. The most dominant effect in the images is created by the change in wind field.

The second group contains images with wind direction between West and North. Figure 10 shows the image of 5 May 2016 when the wind was blowing at 3 m/s from West North West. The image was acquired at evening Utah time, and shows a number of short and linear bright backscatter signals that can be related to boats or ships floating in the lake. The backscatter is lower in the northern and middle region of the lake, which could be related to the wind shield effect of Lake mountain. Also the image has relatively high and homogenous backscatter in the southern region for wind speed of 3 m/s.

Wind conditions at the time of acquisition of 11 July were 7 m/s blowing from West North West (Fig. 11). The image shows high backscatter, but the streaks typical of high wind stress are not as pronounced as was seen for images with winds blowing from South-West direction. A small dampened region can be seen around Mosida point. This dampening could be related to the wind shield effect. However, the 5 May (Fig.10) image with much lower wind stress in the same direction showed no dampening at Mosida point. Secondly, it is a much smaller area than the area under the wind shield effect as seen in all other images. Therefore, alternatively, it may indicate the presence of a bloom at the site.

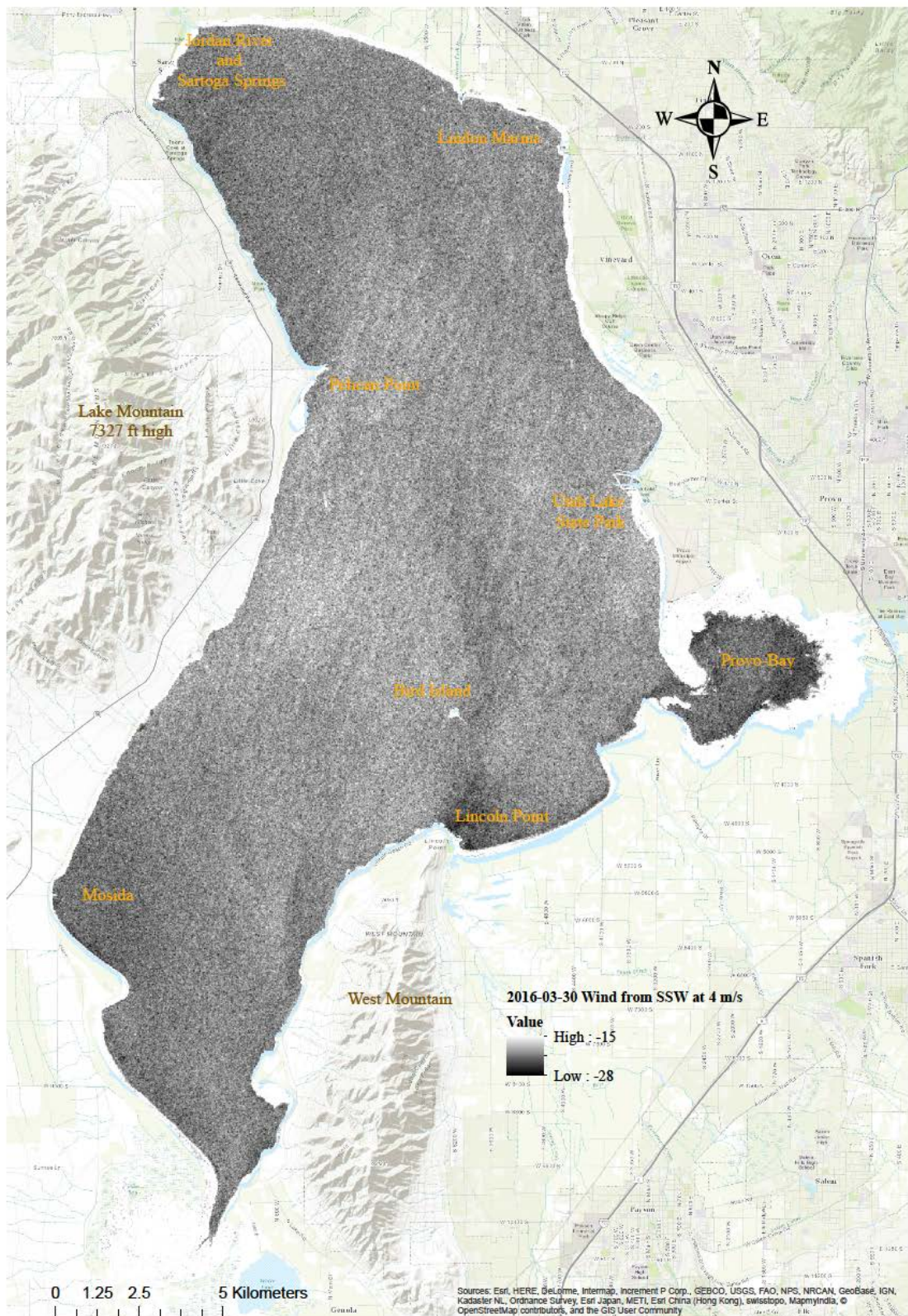Figure 6, C-SAR image from 30 March 2016 for Lake Utah, wind direction ranging between South and West

Figure 7 C-SAR image from 23 April 2016 for lake Utah, wind direction ranging between South and West

Figure 8 C-SAR image from 10 June 2016 of Lake Utah, wind direction ranging between South and West

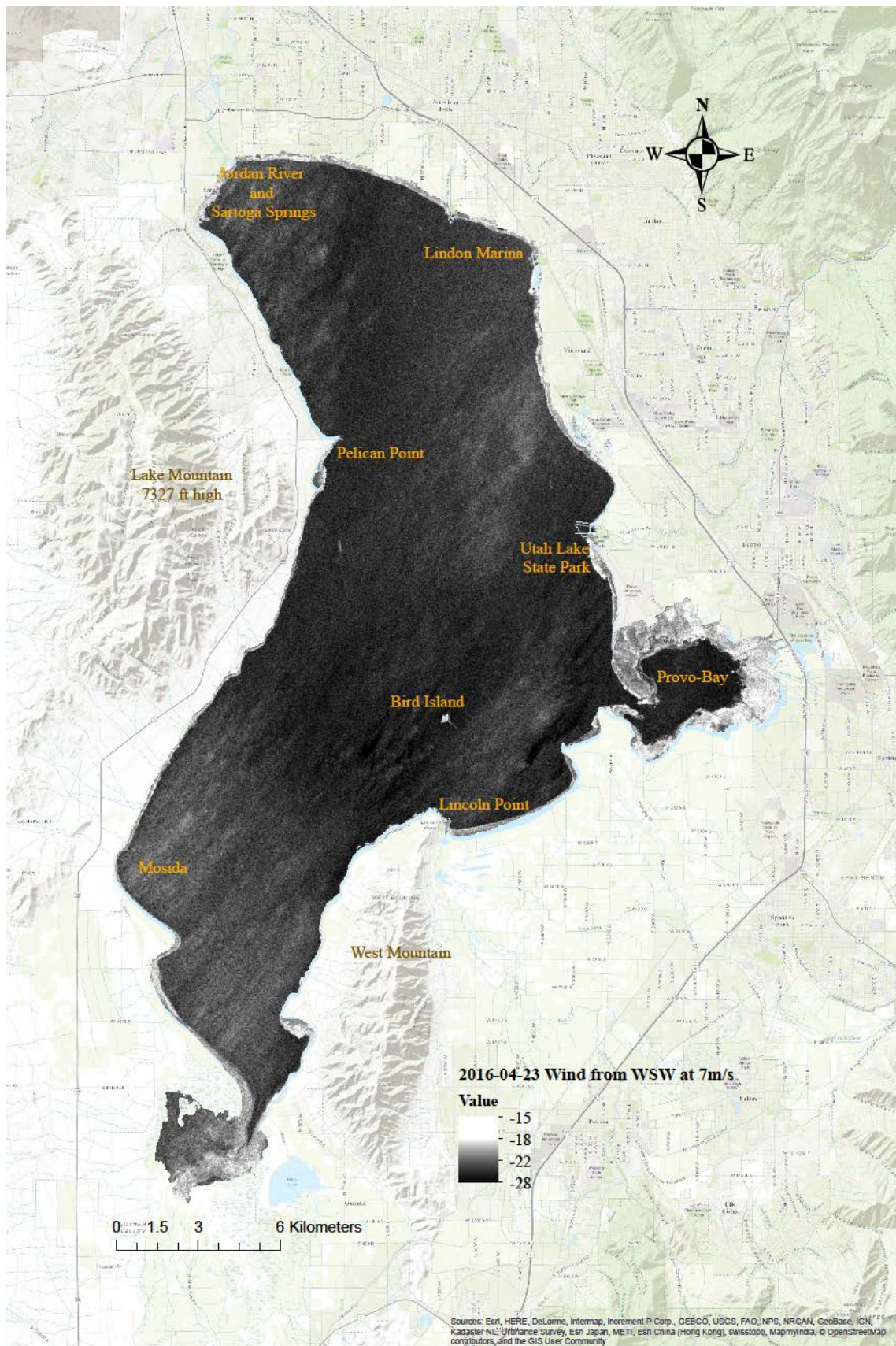Figure 9 C-SAR image from 4 July 2016 of Lake Utah, wind direction ranging between South and West

Figure 10 C-SAR image from 05 May 2016 of Lake Utah, wind direction ranging between West and North

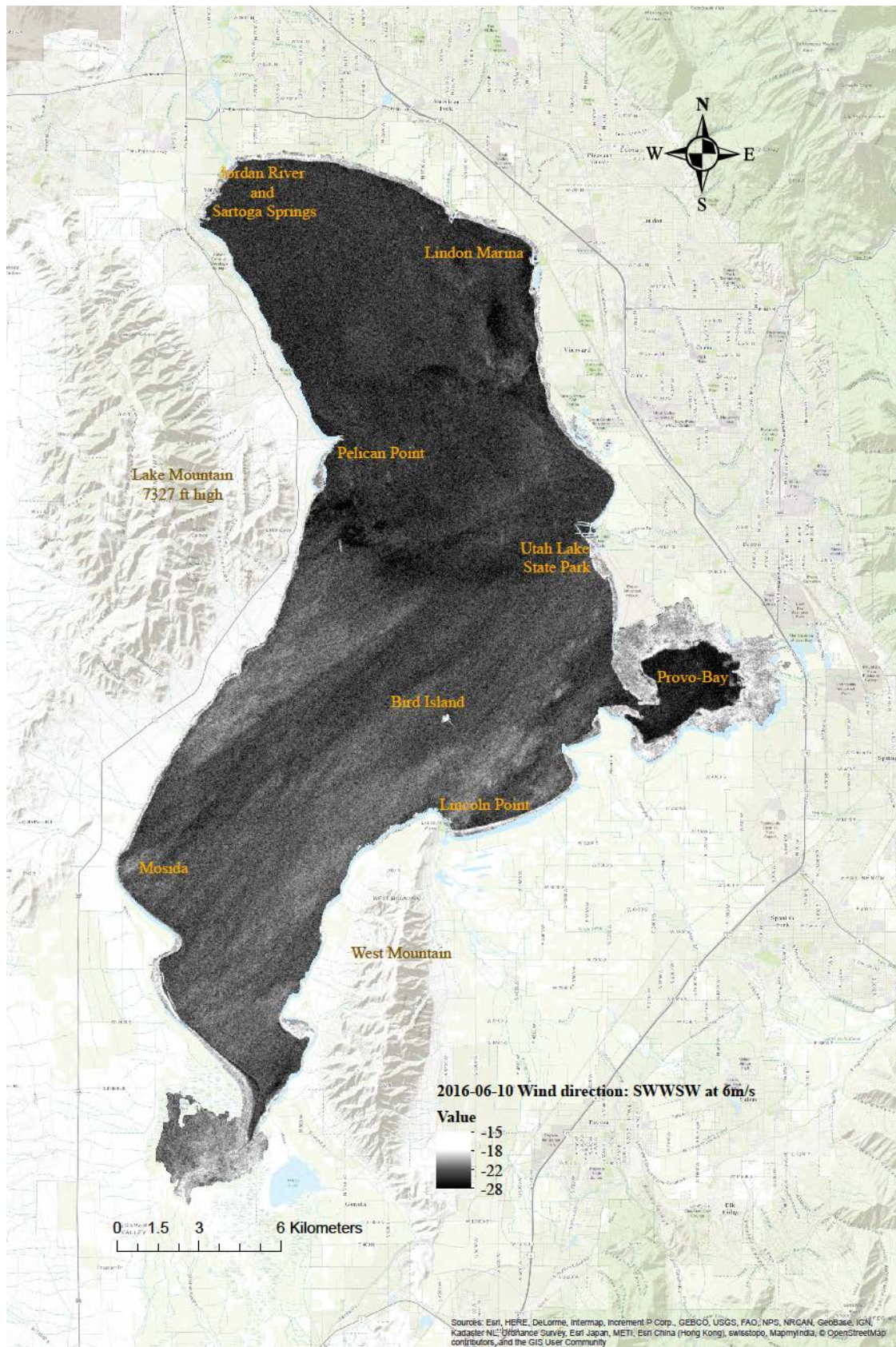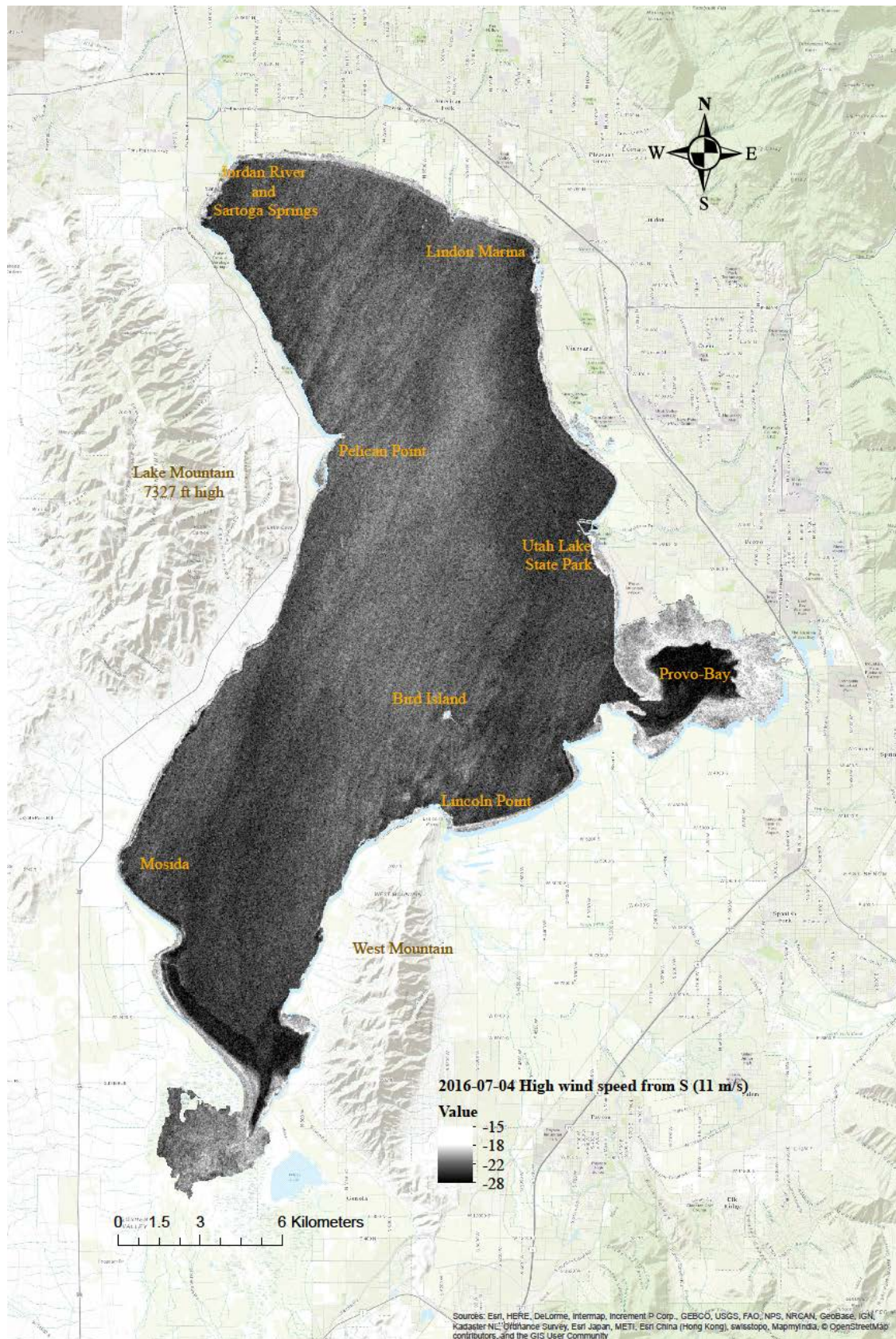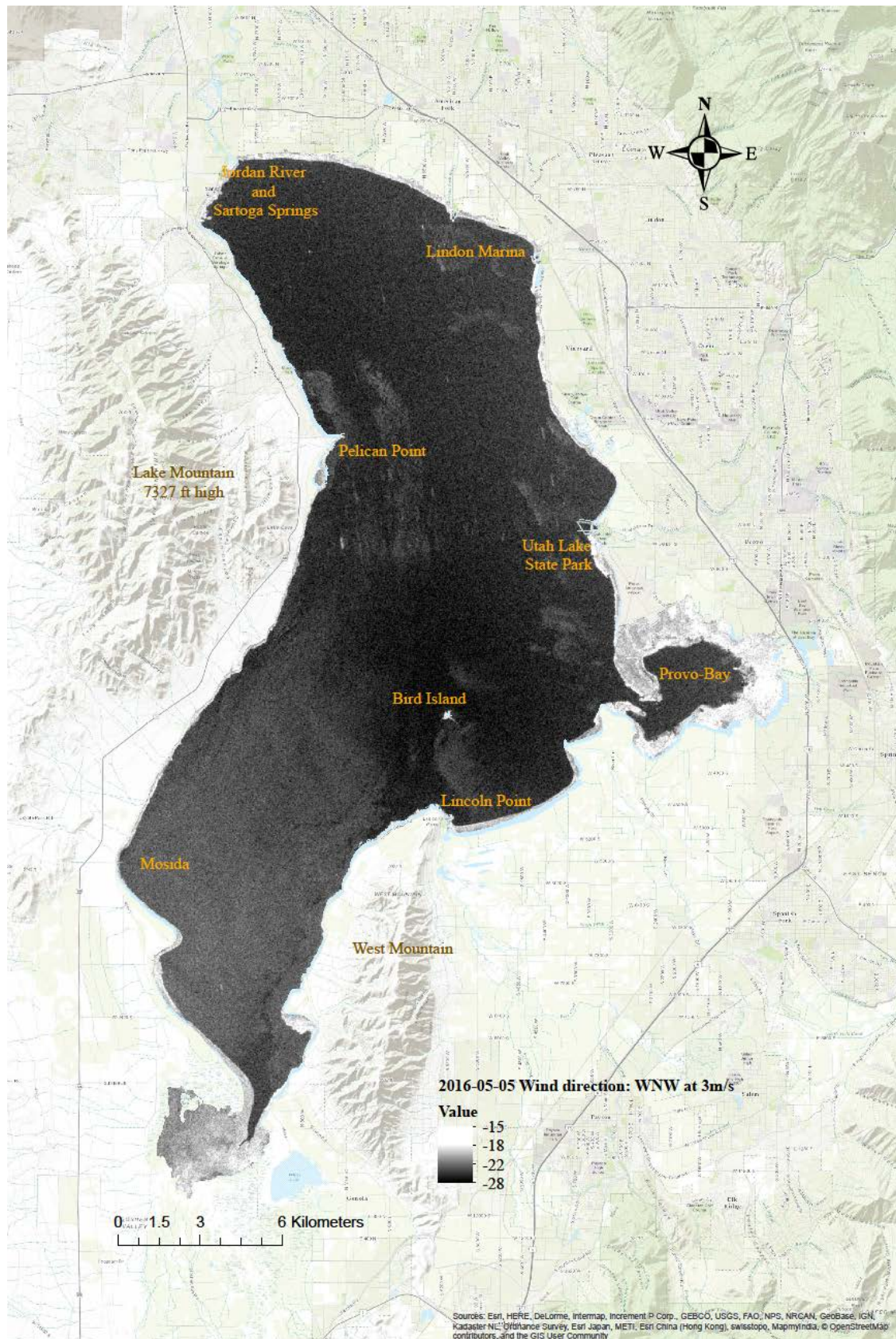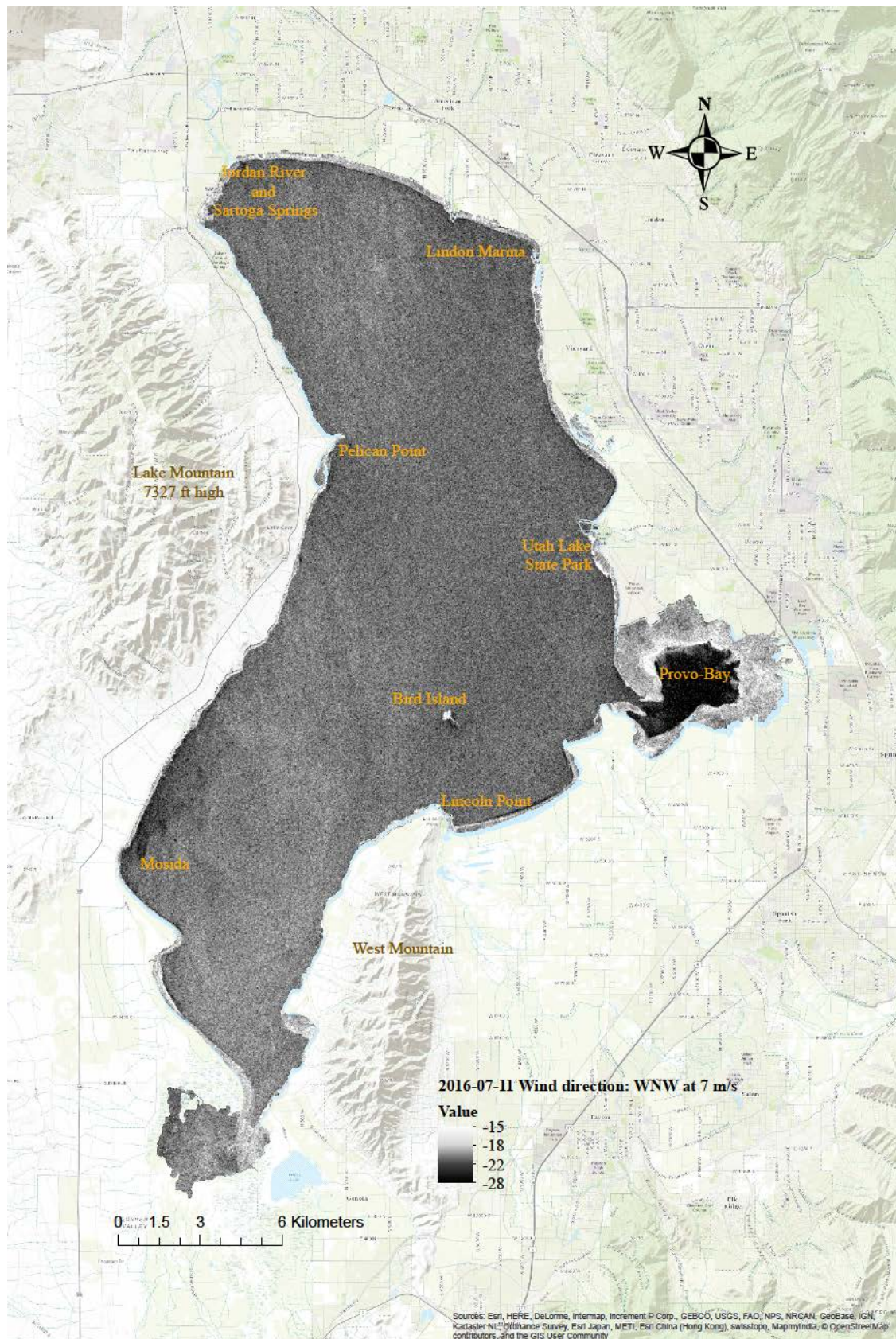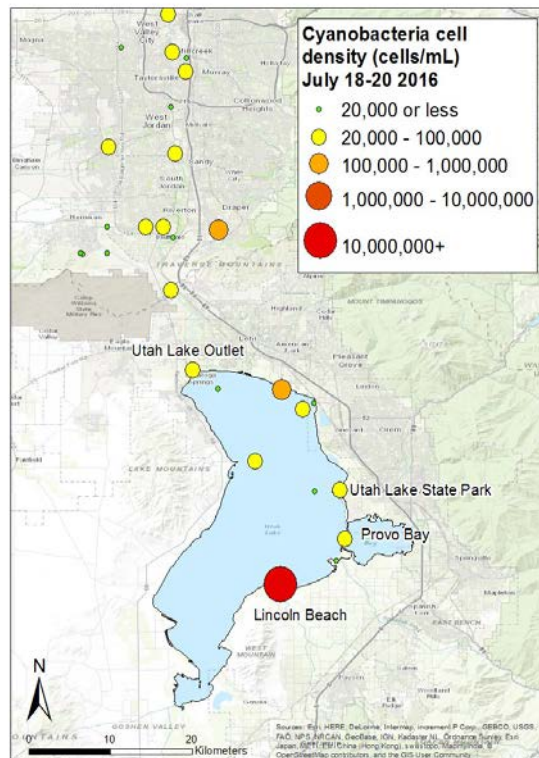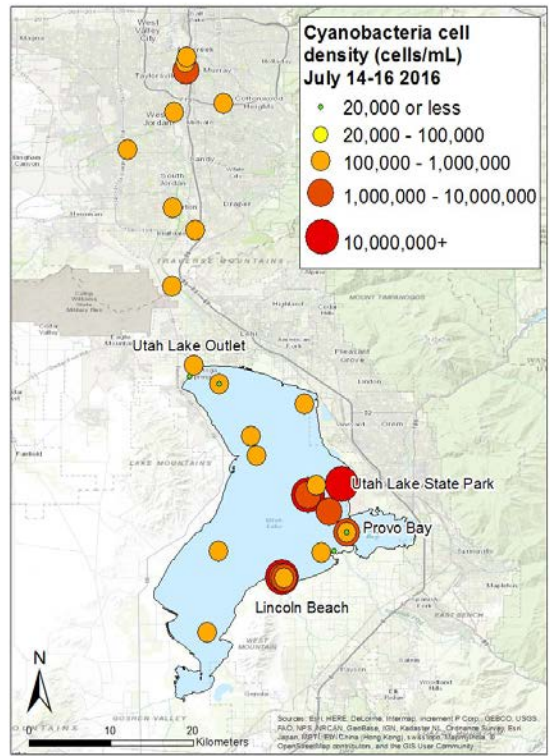Figure 11 C-SAR image from 11 July 2016 of Lake Utah, wind direction ranging between West and North

Figure 12 Algae concentration maps available for Lake Utah for time period between 14 and 20 July. Maps: Official website of Utah lake

The third group of images include an image acquired on 21 July, 2016 at 13:34 UTC time when wind was blowing at 5 m/s from East South-East direction (Fig. 13). This image shows dampening caused by various effects. The dampening along the foothill of West mountain all the way till Mosida point can be related to the wind shield effect of West Mountain. However, the region around Mosida point is supposed to be covered by scums as chlorophyll map derived from optical image from 22 July show very high concentrations of chlorophyll (Fig. 15). If we relate images with similar wind speed but blowing from South-West direction (Fig. 6 & 8) did not show such large scale attenuation in the signal as is seen in this image. This may suggest that the dampening in this region is caused by algae and provide evidence that SAR can sense scums, the floating layers of algae.[6] There is also some dampening at the Lincoln point, above Utah State Park, Lindon Marina and Sartoga springs & Jordan river. These sites correspond to the areas of high concentration of algae in the algae concentration maps from dates between 14 to 18 July (Fig. 12). Also, at the wind speed of 5 m/s the streaks along the wind direction are absent (but Fig. 6 shows streaks from wind speed of 4 m/s).

The maps in figure 12 show decline in the concentration of cells of cyanobacteria from 14 July to 20 July. However, it should be noted that it is not clear if the samples were taken from the water column or the water surface. Nevertheless, multiple forms of evidence from July show very high concentration of algae at the dampened sites in C-SAR image from 21 July (Fig. 12 & 14). Another form of available validation data is the optical image acquired on the day after (22 July, 2016 at 18:21 UTC time). Figure 15 is chlorophyll concentration map derived from Sentinel-2 imagery shows high concentration of algae around Mosida, Utah State park and Sartoga springs. It does not show the high concentration of algae at Lindon Marina, even though the data from previous days show high algae infestation at the site (Fig. 12 & 13). One explanation could be that the bloom moved away from Lindon Marina in the time between the acquisition of C-SAR and optical image.

---

[6] The algorithm used to create this image produced no data, this limitation of the optical image is discussed in section 3.2.
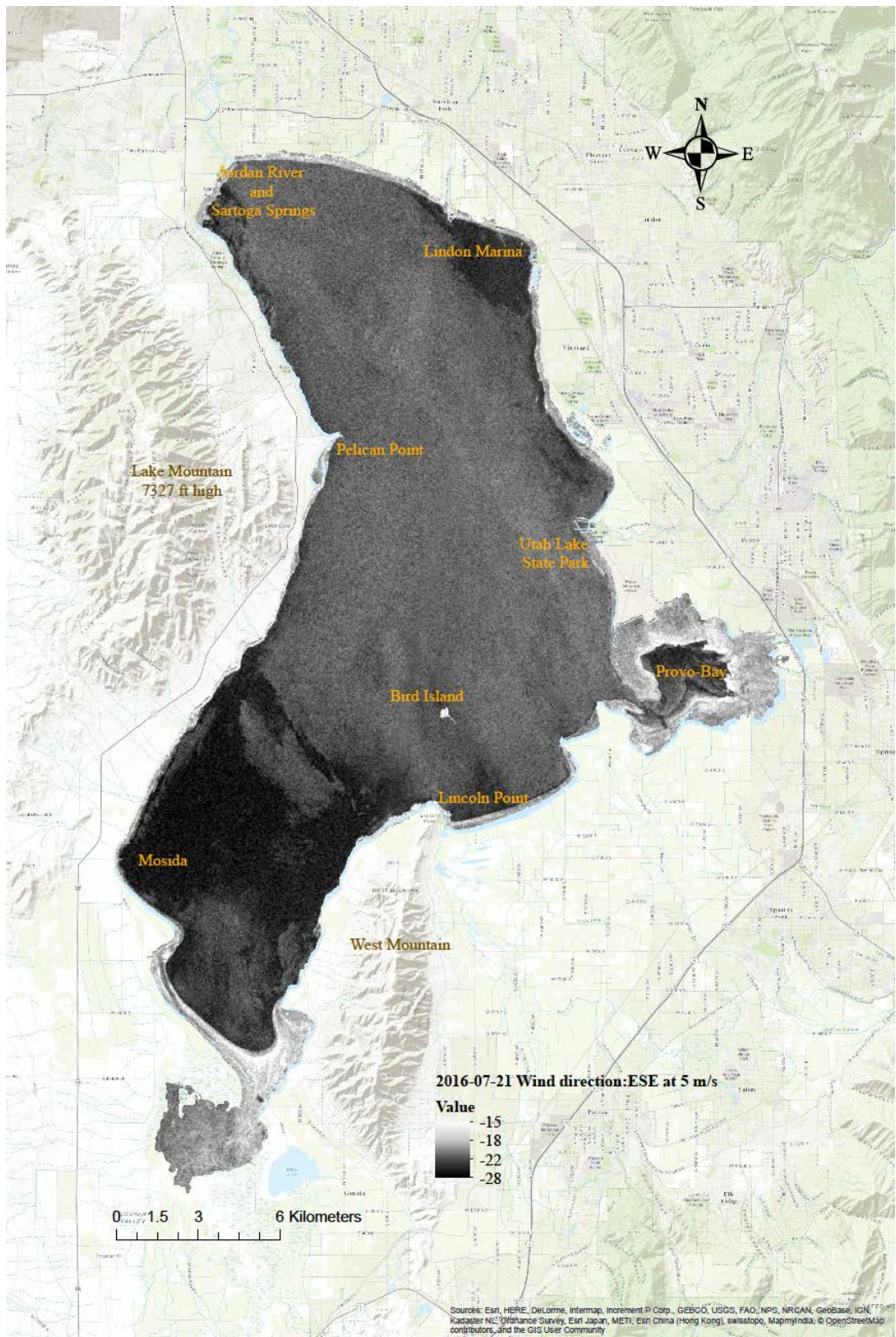
Figure 13 Wind direction ranging between East and South, Lake Utah image from 21 July 2016 at 13:34 UTC time
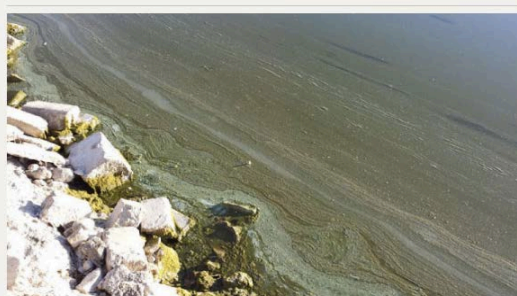
Courtesy of Utah County Health Department Toxic algae is being blamed for a dog's death at Utah Lake.

Single page

Stay out of the (scummy) water.

That's the word from the Utah County Health Department, which reported Tuesday that a dog died over the weekend after playing at Utah Lake's Lindon Marina and drinking water contaminated by blue-green algae toxin. The algae, cyanobacteria, are sometimes called "pond scum."

After Utah Lake-related dog deaths, experts recommend protocol for toxic algae

By EMMA PENROD The Salt Lake Tribune

First Published Jul 30 2015 07:15PM   Last Updated May 05 2016 08:35 pm

Figure 14 News article scums at Lindon Marina kills a dog from weekend before 30 July. Photo: Salt Lake Tribune

Colour	Value
	0
	20
	40
	60
	80
	100
	120
	140
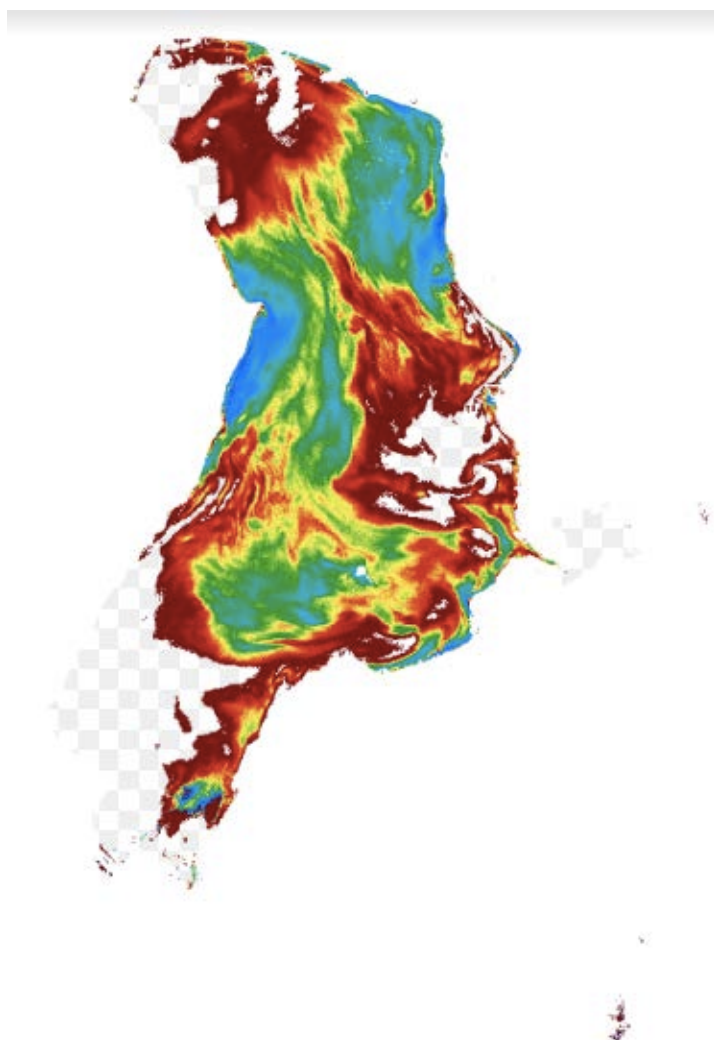
Figure 15 Chlorophyll classified optical image from 22 July, 2016 at 18:21 UTC time. (the blanck values are higher than 500 μgl^{-1} and the white shows the presence of clouds) Image: Annelies Hommersom, Water Insight

The next group belongs to images acquired at the time of changing wind conditions. Often it is changing wind direction accompanied by low wind speed (less than 3 m/s). These images show patches of high and low backscatter. The figures 16 and figure 17 were acquired on 16 April and 24 May 2016, respectively. The wind had been blowing from North at about 3 m/s half an hour before the acquisition of the image in figure 16 and fifteen minutes after the acquisition the weather station showed calm conditions. For 24 May, the wind was blowing at 2.1 m/s and the direction changed from West North-West half an hour before acquisition to frequently changing directions half an hour after the acquisition of the image (Fig. 17). The image from 28 July was acquired under slightly changing wind conditions (Fig. 18). The wind direction changed from North-North-West to West and the speed declined from 4.1 m/s to 3.6 m/s.

It is observed that under changing wind condition the water surface witness an uneven wind stress, which causes random patches of high and low signal on the image. Images acquired during the changing wind conditions displayed patterns that might be related to wave swells (around the deeper regions), swirls and waves breaking (around the edge of the lake). These patterns were abrupt and were visible as spiral and sweeps of dampened regions or wedge shaped brightened regions. This can be attributed to the fact that changing wind conditions coupled with surrounding topography altered the wind directions and speed. This led to wind tunneling effects in some regions and wave shield effects in other regions. For example, high wind speed in shallow regions causes waves to break or wave swirls in case of a sudden change in wind direction. While high wind speed in deeper regions causes wave swells. These could be described as the symptom of unstable wind stress. The figure 18 from 28 July shows the effect less severely than the other ones (Fig. 16 and Fig. 17). This could be related to the wind speed, as wind speed in figure 18 was higher than the wind speed in the other two images. Alternatively, it could be related to the presence of algae, which prevented a sudden change in water surface structure making it relatively more resistant to changing wind stress on the surface.
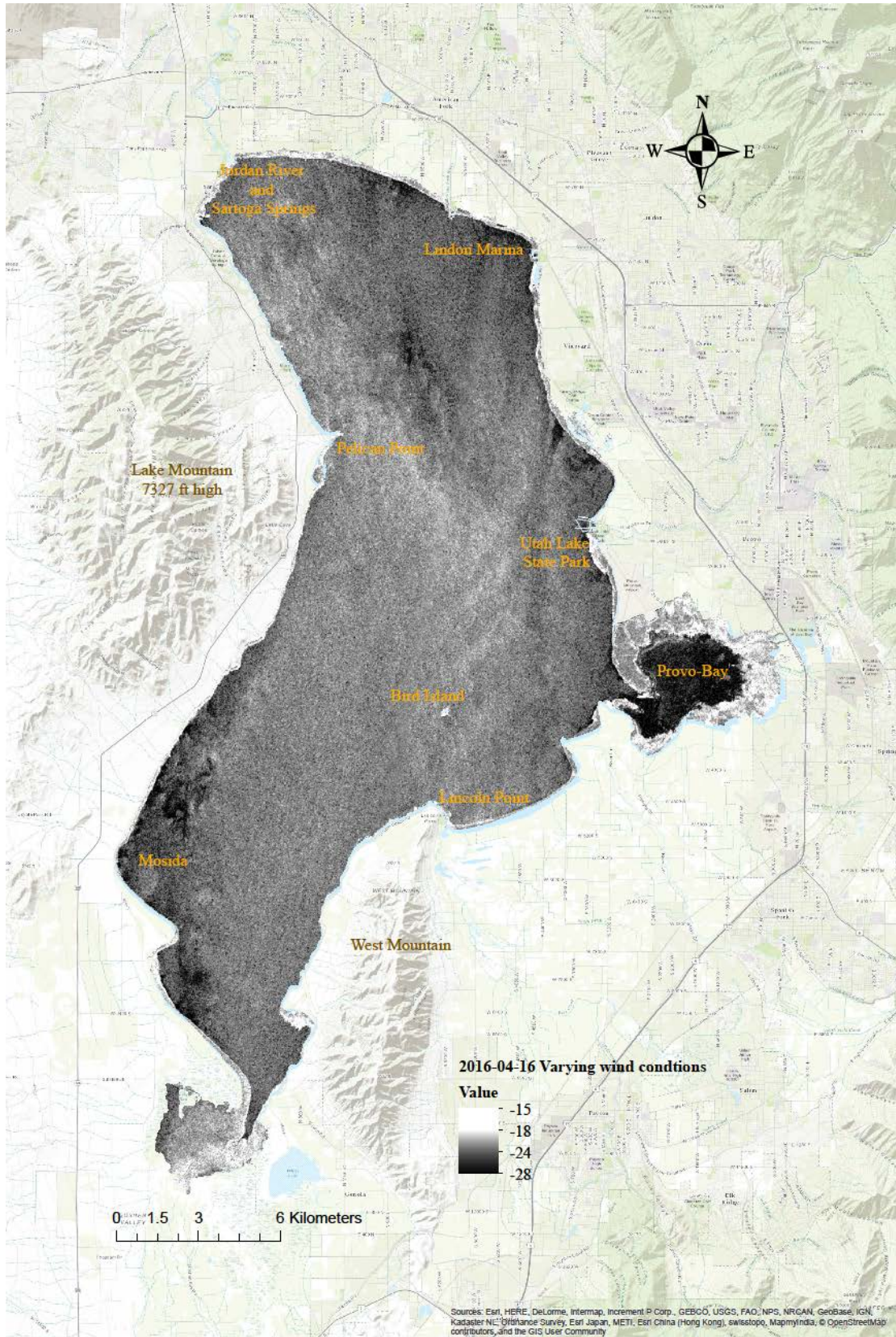
Figure 16 Under changing Wind conditions, Lake Utah image from 16 April 2016
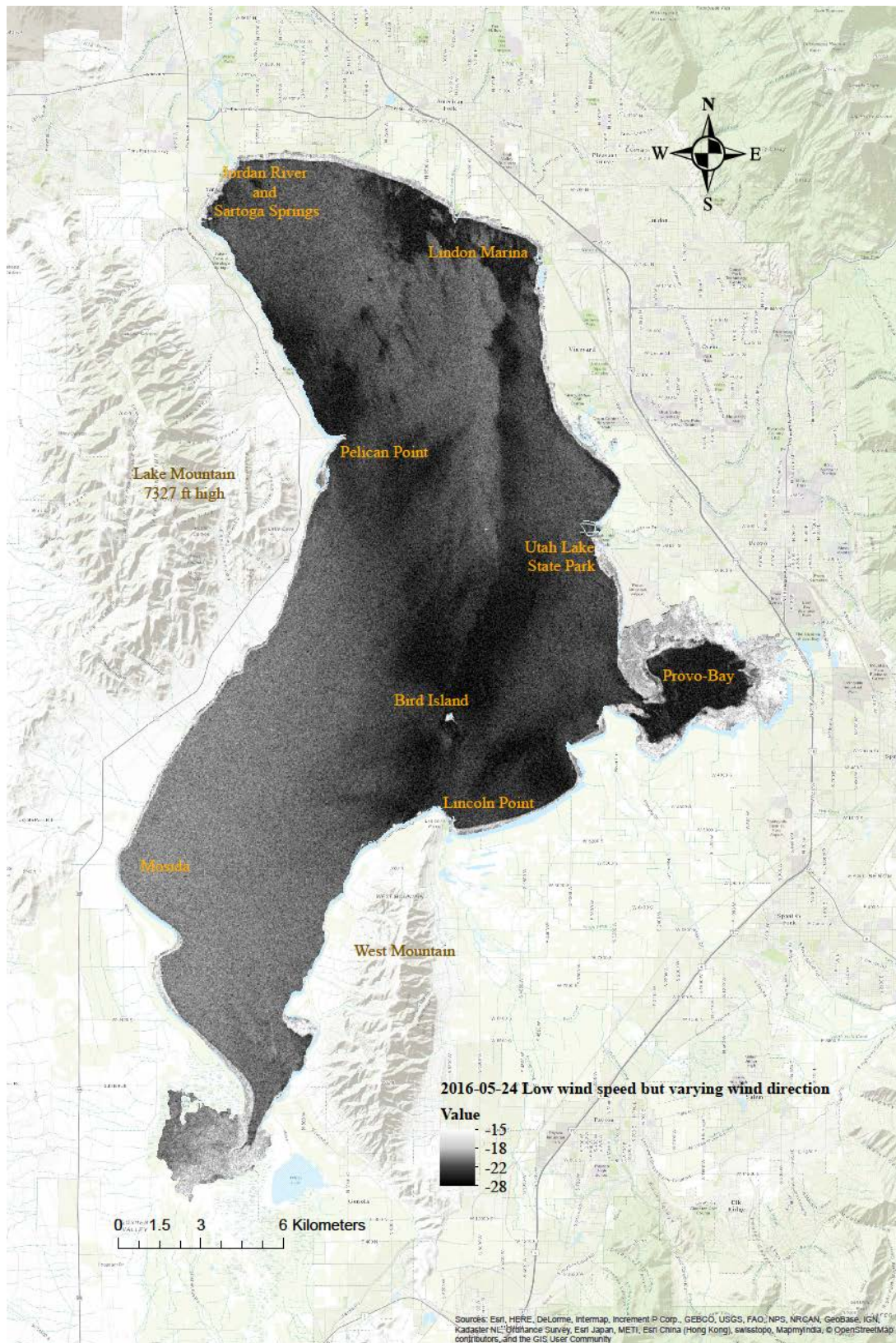
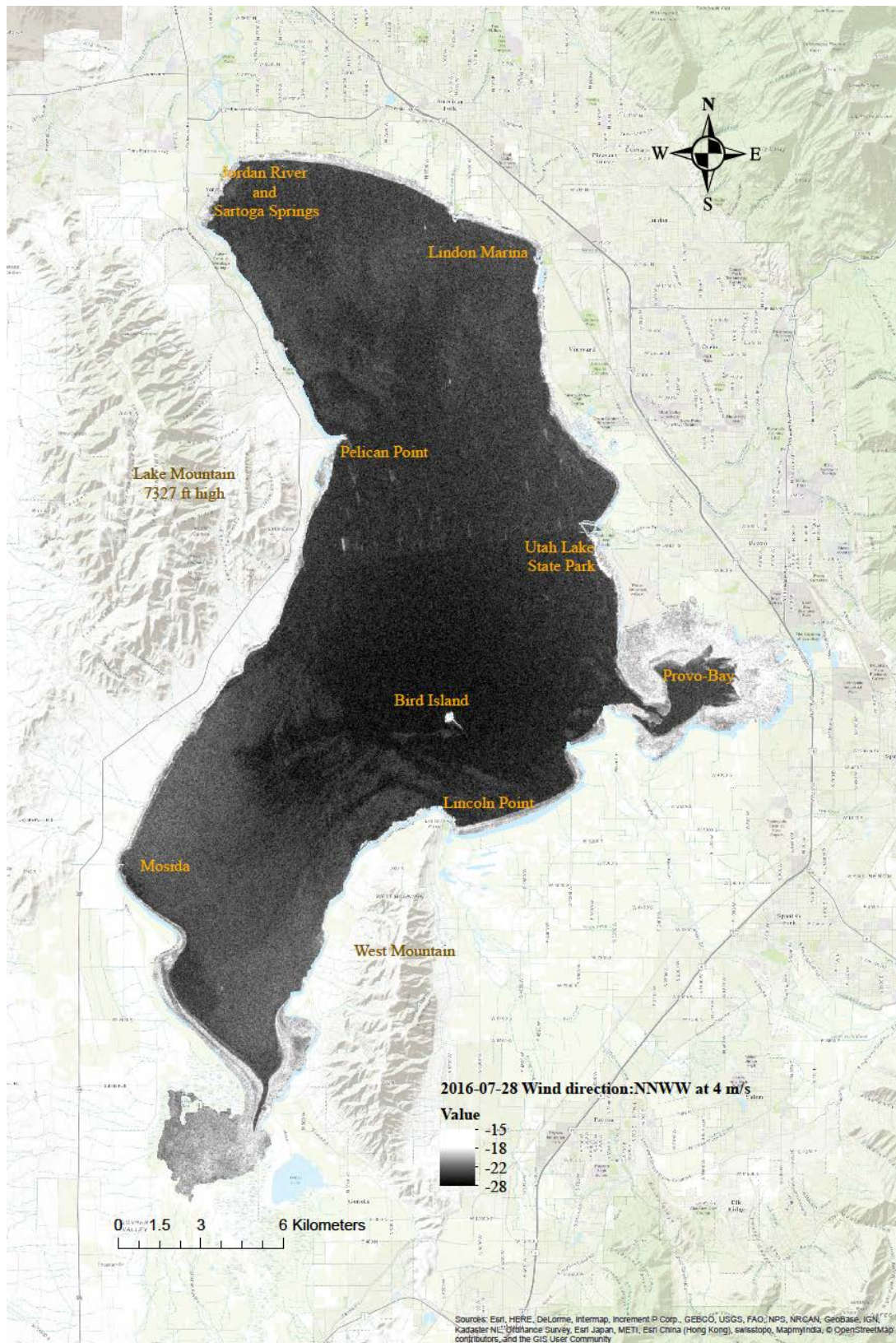Figure 17 Under changing Wind conditions, Lake Utah image from 24 May 2016

Figure 18 Under changing wind conditions, Lake Utah on 28 July 2016
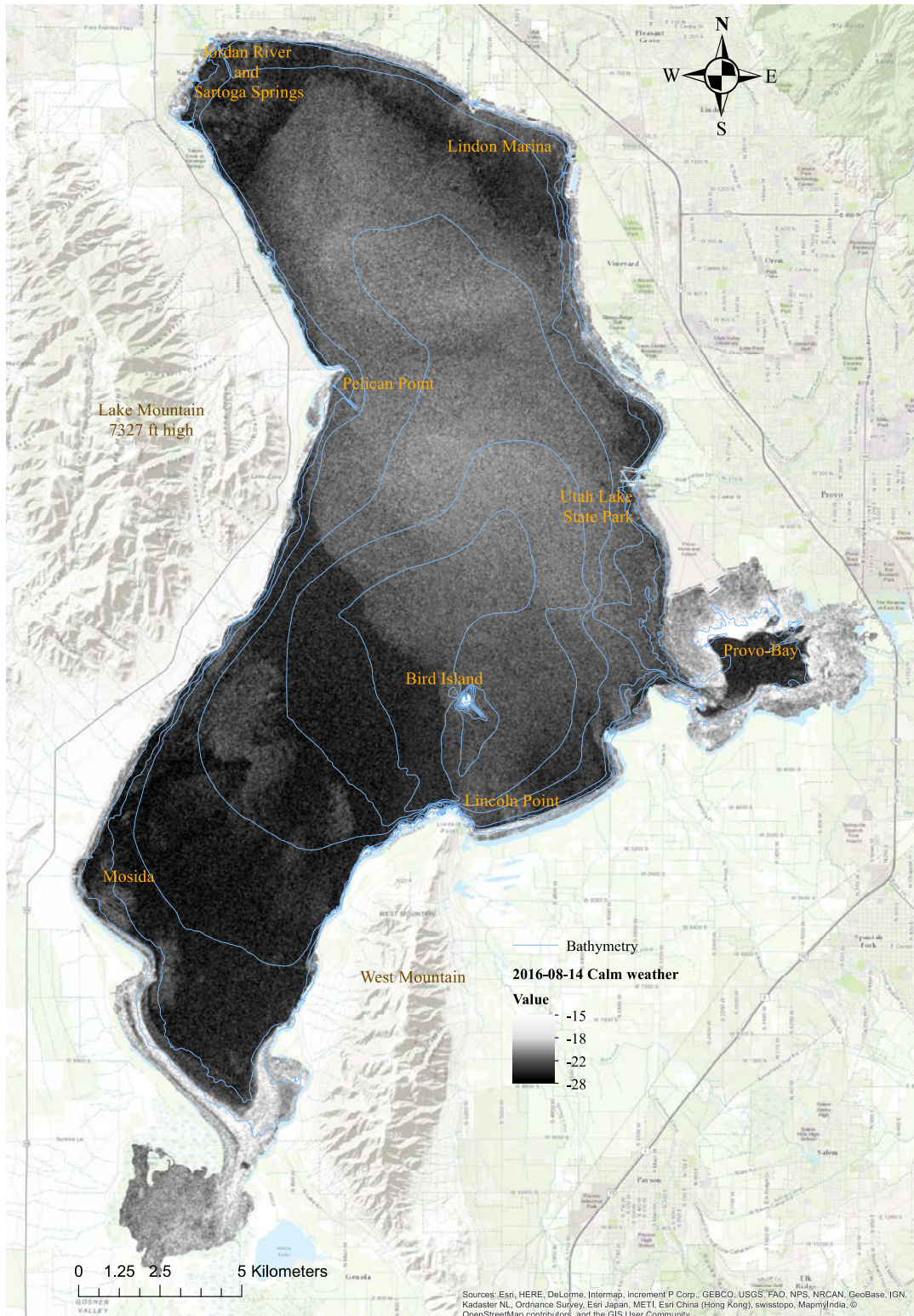
Figure 19 Image from 14 August under calm weather conditions with an overlay of lake Bathymetry

The last group includes C-SAR image acquired on 14 August under completely calm conditions (Fig. 19). On 14 August the wind conditions were completely calm and the wind records showed no sign of wind for at least two hours before acquisition of the image. In contrast to the expectation that completely calm conditions would lead a very low overall backscatter, there are still structures visible on this image. The northern part of image shows structure that somewhat agrees with the lake bathymetry. However, this can not be said for all the structure present in the image. There are probably more unknown factors acting on the surface.

Having analyzed the Utah lake images the following hypotheses are put forth:
a. Backscatter in the C-SAR images is in general related to the wind speed recorded at the nearest weather station. However, this relationship is not linear (as seen in the results from images acquired with wind direction between South and West). The wind stress at different regions of the lake is different depending on the surrounding structure.
b. C-SAR images captured during the time of low wind speed and changing wind direction show high backscatter in some regions. Low wind speed appears to manifest differently in C-SAR images as opposed to conditions when the wind stress is higher and stabilized. Also, under completely calm conditions, the backscatter is still visible and can be partly related to the bathymetry that dominates the flow of water from an inlet or a wind gust, or to a long duration of high wind stress that may have developed swell waves across the lake.
c. Algae infestation in C-SAR manifests as a gradually dampened region and often around the border of the lake close to the region suffering from an algal bloom.
d. Presence of algae may prevent the formation of water turbulence under changing weather conditions.
e. Local shields may cause local changes in the wind shear stress. This may cause difference between actual and recorded stress at a weather station.
f. It is also seen that not all structures in the image can be explained. The C-SAR images sometimes show sensitivity to changes that are hard to measure, probably local and lasting few seconds.

4. 2 Results from lake Paterswoldsemeer

Quantitative analysis was performed for lake Paterswoldsemeer. Firstly, a reference site was chosen, which is shown in figure 20 as red circle. It was based on the radius of the circle around the point. It generated the maximum possible fetch in all directions.
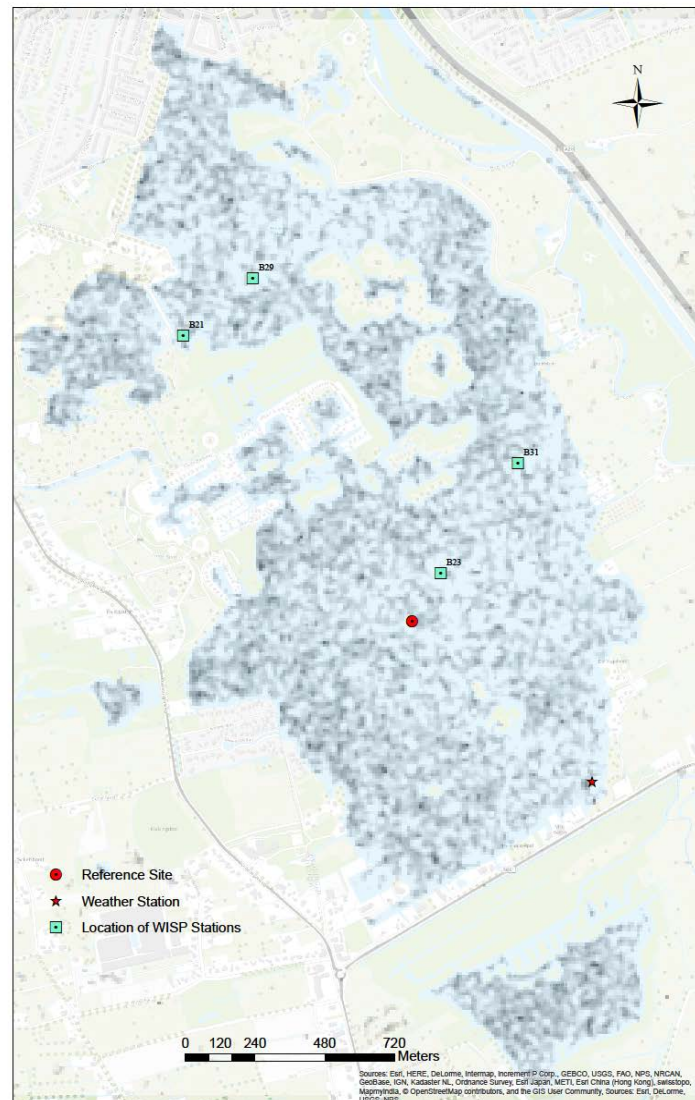
Figure 20 A C-SAR image overlay on topographic base map with reference site, weather station and WISP station sites for Paterswoldsemeer

Next, an 11x11 square pixel window was chosen to average the signal at a location. The figure 21 shows the gradual increase in the stability of the backscatter signal as the size of the window increased from 3 to 11.

Backscatter with 3x3 window
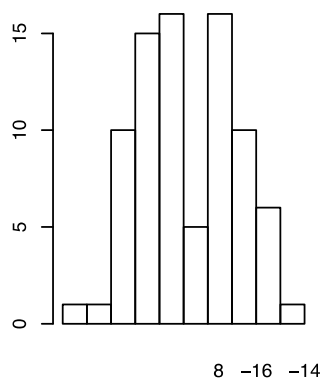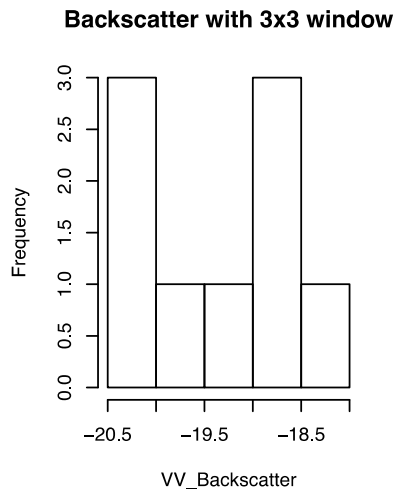
Figure 21 Stabilization of signal for a randomly chosen WISP station site with increase in window size

The trend of the backscatter signal and the wind speed along discreet time stamps can be seen in figure 22. For most time stamps, a high backscatter is accompanied by a high wind speed. With decrease in wind speed the backscatter signal also tends to decrease. There appear to be additional factors other than wind causing change in backscatter for time between 30 June and 10 August 2016. For 27 July, a wind speed of 2 m/s was recorded at the weather station but the backscatter received from the reference site is higher than -20 db. The disturbed relationship for these moments may be attributed to increase in recreational activity at the lake during the month of July.
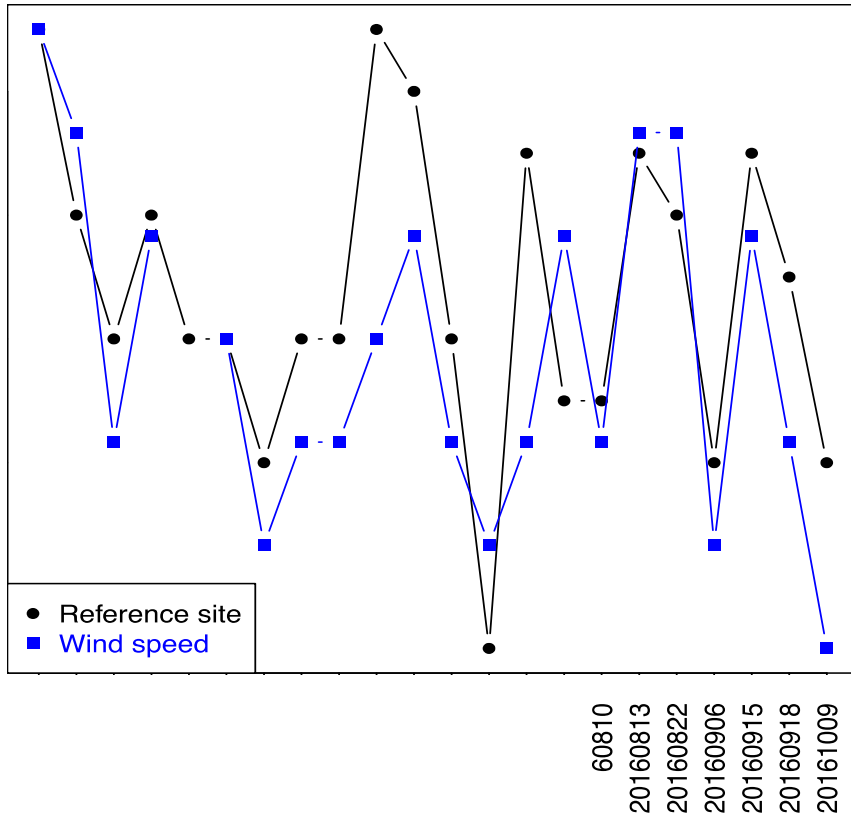
Figure 22 Backscatter at reference site with wind speed plotted on the other axis

The temporal distribution of the backscatter signal measured at the WISP stations B31, B29 and B21 is shown in the figure 23, figure 24 and figure 25, respectively (refer Fig. 19 for wisp station locations). The reference site is also plotted in the same plot to see if the changes might be caused by local factors. The three WISP stations are located along the northern part of the lake and were most severely hit by algal blooms. The distribution shows that the backscatter signal for the time period when the lake was free from algae was high for high wind speed and low for lower wind speed. For most time stamps, the backscatter trend line follows the backscatter at the reference site.
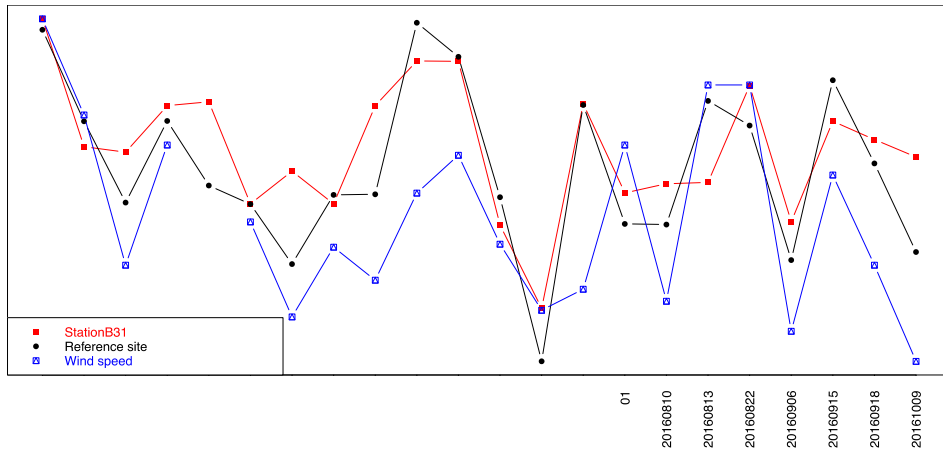
Figure 23 Backscatter observed at WISP station 31along with the backscatter recorded at the reference site
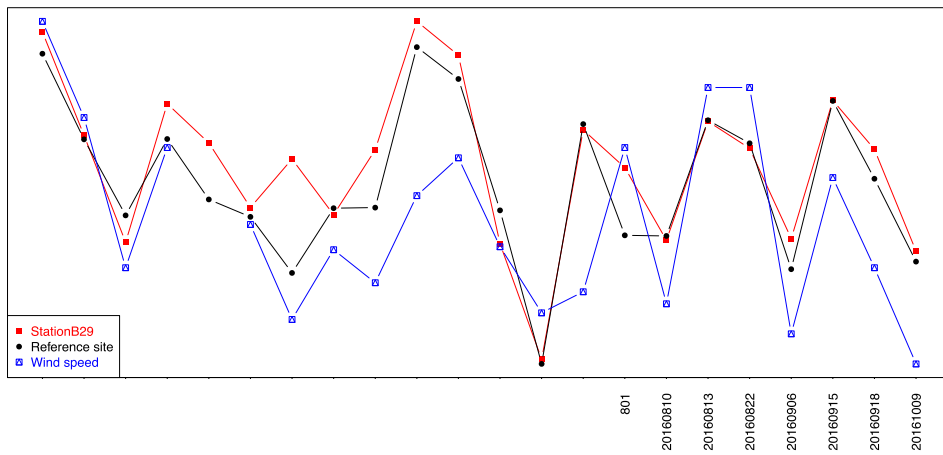
Figure 24 Backscatter observed at WISP station 29 along with the backscatter recorded at the reference site
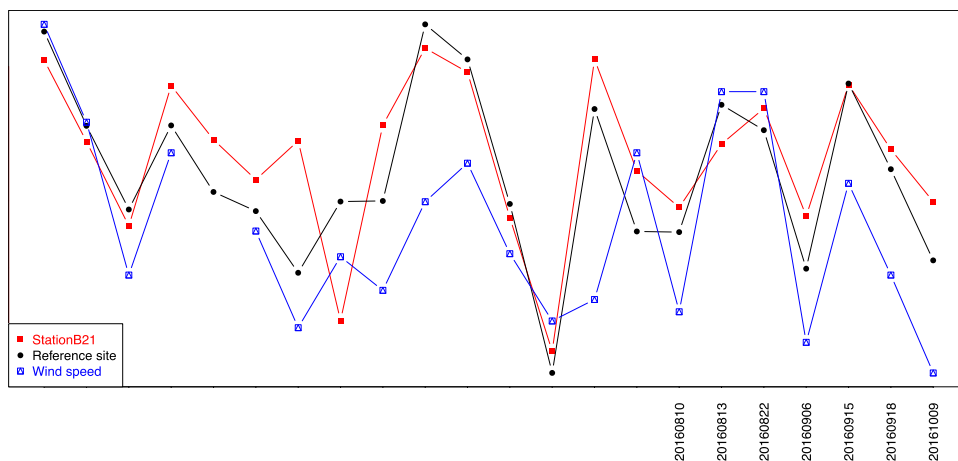
Figure 25 Backscatter observed at WISP station B21 along with the backscatter recorded at the reference site

Backscatter, from the month of June, starting with the image taken on 11 June, 2016 till images from the month of August (with an exception of 1 August, 2016), did not follow the trend line of wind speed. These images show a different effect as they show a high backscatter, which could not be explained by the wind speed. This is true for all the three WISP stations and the reference site. This does not follow the expectation of a dampened backscatter signal for the time when the lake suffered from an algal bloom.

Backscatter at WISP station B31 for 27 July is particularly interesting (Fig. 23). Backscatter is as high as it was observed for high wind speed of 6 m/s in the image captured on 31 January 2016. But the wind conditions for 27 July indicate a low wind shear stress. Therefore, it can be concluded that the high backscatter was not the result of wind shear stress at these stations but due to other factors.

For WISP station B21 (Fig. 25) the backscatter for 30 June 2016 is lower than it can be expected from the wind stress observed at the site. While for the other two WISP stations for this date, the observed backscatter is in line with the wind shear stress.

Also, at stations, B29 and B21 (Fig. 24 & Fig. 25), backscatter on 1 August is higher than it is observed at the reference site, thus becoming closer to the 'original' relation with the wind speed.

Figure 26 The bloom seen on 27 July 2016 between station B 17 and B 31. Photos by BlueLeg Monitor

Photographs were available for 17, 20 and 27 July 2016 and captured algae present in the water in the form of both intense algal bloom and scums at the sites. The bloom was one unit (homogeneous) and spread across a few hundred

meters (personal communication with the student at BlueLeg Monitor who carried out the fieldwork and made the photos of figure 26). The white foam in the figure 26 indicate the presence of scum, which were much smaller than the subsurface bloom. The expert of the water authority Noorderzijlvest (responsible for lake Paterswoldsemeer) explained that the lake had more than 100,000 visitors a week during the month of July. Being asked about the presence of the boats, the answer was "there were many, many boats everyday on the lake". For all three dates, C-SAR received high backscatter except for 24 July 2016. The low backscatter may be caused by the presence of scums but the available data to shows otherwise. The exceptionally low backscatter on 24 July was observed across the whole lake (at reference site) and not just at the WISP station 31, this eliminates the possibility of low backscatter from scums. Also, the possibility of low backscatter on 24 July as an effect of algal bloom can be eliminated by the very low wind shear stress recorded for this day.

If the chlorophyll concentrations from WISP hyperspectral data are plotted along with VV-backscatter for WISP B31 no particular relation can be derived from it (Fig. 27). High backscatter was observed for days when chlorophyll levels (proxy to algae) were also high for this site.
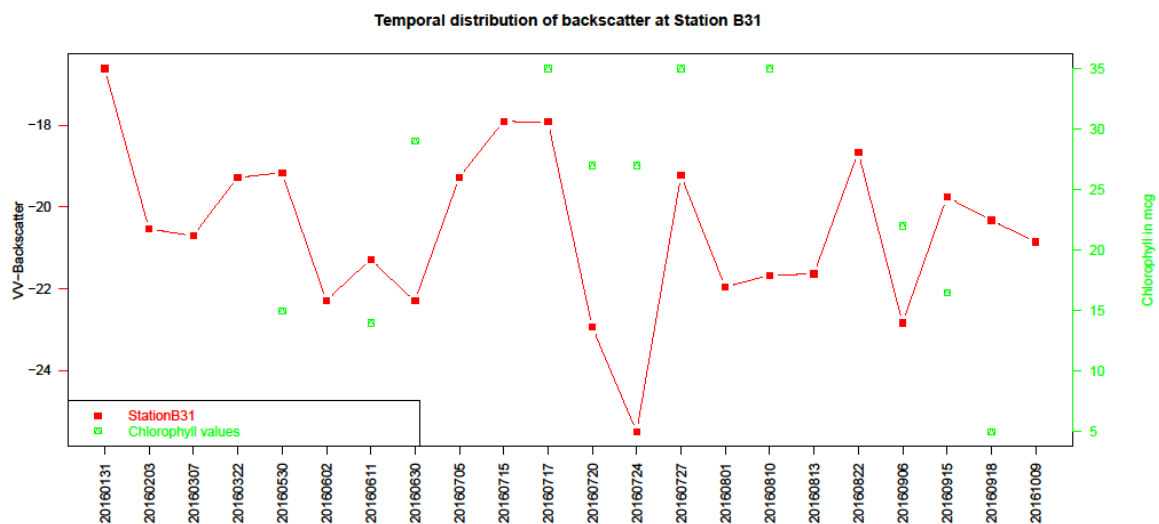
Figure 27 Backscatter observed as opposed to the chlorophyll values
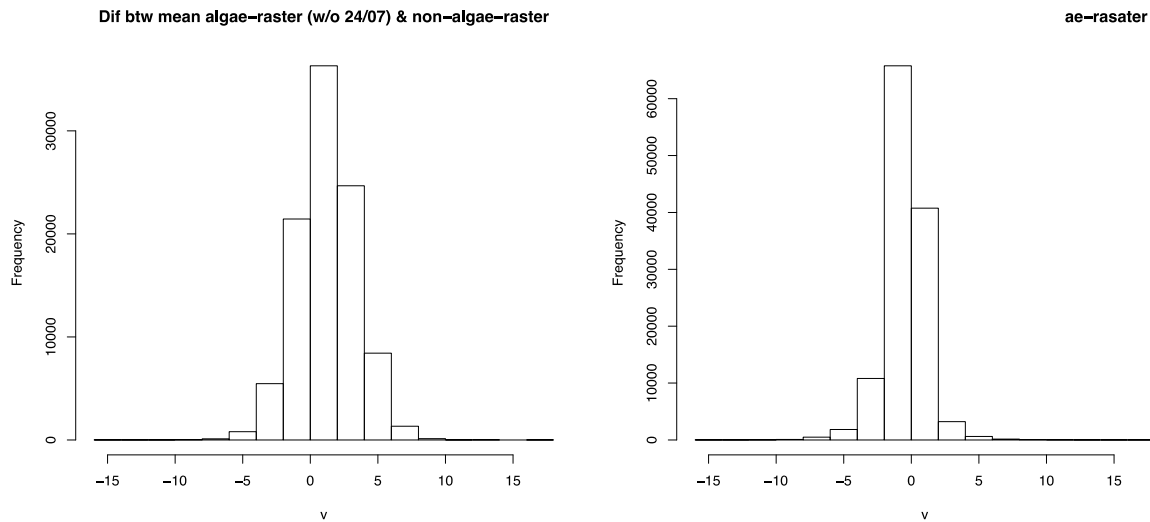
Figure 28 Histogram of all pixels in raster created by subtracting mean radar signal from images with algae and mean raster from images without algae.

In order to see if C-SAR images can provide more information when grouped together as compared to information from an individual image, all images were divided in two groups. One group contained images when no algal blooms were present and the second group when there were algae infestation in lake. The average per pixel backscatter value for the group containing images from the time when the lake suffered from an algal bloom was lower than the average per pixel backscatter for the second batch containing images from the time when the lake was free of algae. However, the decrease in the mean backscatter for time of algae infestation was due to the outlier image from 24 July 2016. On this day the backscatter was showing the lowest signal and behaved as an outlier which lowered the mean backscatter for the batch. After excluding this image for mean fcomputation, the average backscatter per pixel for the two batches showed higher backscatter for the time period with algae infestation. As can be seen in two histograms in figure 28, the difference between mean raster from algae infestation period and mean raster from algae-free period is inclined to the positive values (left) when 24 July is removed from the mean raster from algae infestation period (mean-algae raster > mean no-algae raster). But when 24 July is included in the mean raster for algae infestation period more values are inclined to the negative difference (mean-algae raster < mean no-algae raster).

4. 3 Summary of results

For lake Utah, the algae infested areas were observed as dampened regions in C-SAR images where the wind stress was relatively higher over the lake surface. It was observed that high wind speed, more than 5 m/s creates a stable wind stress on the lake surface that dominates over any other factor that might influence the backscatter. The high wind speed cause waves pattern to stabilize and orient itself towards the wind direction. Under changing wind direction, C-SAR images along the lake borders show wave breaking and backscatter from unexplained factors. Backscatter in such images was not homogenous on the lake surface but random sweeps of dampening regions were observer. The C-SAR image did not show wave swirls or breaking along the edge under changing wind conditions at the time of algae infestation. Also, under calm conditions other factors came to play in influencing backscatter. In the absence of stable wind stress (from high wind speed), the wind losses the domination and various other factor come to play in influencing the change in backscatter.

The first hypothesis established from lake Utah about the relation of backscatter signal with the wind stress is also seen for lake Paterswoldsemeer. The results from lake Paterswoldsemeer also showed that factors other than wind stress influenced backscatter signal. However, dampening in algae infested regions was not observed for lake Paterswoldsemeer. On the contrary, the backscatter signal from algae infested regions was much higher considering the wind stress experienced by the lake. The results from the two lakes were very different from each other. Most of the experience from lake Utah was not confirmed for lake Paterswoldsemeer.

Chapter 5: Discussions

This chapter is divided in three sections. In the first section, the limitation of the data used in the study is discussed. Section two presents a critic on methods used in this study and existing knowledge on sensing lakes in radar images. In the last section, results of the study are discussed.

5. 1 Discussions on the site selection and available data

The selection of study sites is a crucial step in an exploration study. The aim of this study was to carry forward the existing literature on sensing algae in C-SAR images of an average lake. Two lakes were selected: 1) Lake Utah, which suffered severe algae infestation in summers 2016 and 2) Lake Paterswoldsemeer for which most firsthand validation information was available. The two sites share little similarity. The differences offered challenges of facing different processes at two sites. But they also allowed an insight on factors crucial to actualize the monitoring of algae in lakes using C-SAR images. So far, studies on monitoring of algal blooms in radar images used study sites, which are much larger than those selected in this research. The two most recent researches in the field, sensed algae in Curonian lagoon of Lithuania and Lake Taihu of China (Wang, Li, Bing, Qian, & Zhang, 2015; Bresciani, et al., 2014). Curonian lagoon is more than ten times the size of lake Utah, and Lake Taihu is more than twice the size of the Curonian lagoon. Since most literature is concentrated on radar remote sensing of water surfaces of oceans and seas, the studies on lake reproduce the principles and model applied for seas to study lakes. For large inland water bodies such as a Curonian lagoon it is easier to approximate the forces acting on the surface to that of forces that are at play on sea surface. In this study, lakes of much smaller size are observed.

Lake Paterswoldsemeer is a very small lake (less than 2 km^2), which requires the highest possible spatial resolution. Therefore, Sentinel-1 is selected as the key source of data in this study. The Sentinel-1 satellites (a & b) have a high spatial resolution (10 m) and a high revisit time of 6 to 12 days but in this study only images of Sentinel-1a could be used. The size of lake Utah on the other hand is much larger (370 km^2), where slightly coarser data would not have

affected the study. But consistency in data source is necessary if the results from one site are to be tested at another site to remove differences that may originate from the data source. Yet another motive of the study was to witness a complete growth cycle of algae in one season so that the changes can be linked to the growth dynamics of algae. This exercise demanded high temporal resolution of the dataset especially at the time of algae infestation in a lake, which was possible with Sentinel-1 dataset.

Validation data for Paterswoldsemeer was in-situ data from the WISP devices of Water Insight. The sites where WISP stations are installed for data collection were mostly along the edges of the lake and therefore, a complete picture of spatial distribution of algae was missing. The data, however, provided better picture of algal blooms distribution in time. The information about algal blooms in Lake Utah was also not spatially and temporally complete. Literature has shown that time is a very critical factor in sensing algae, especially the harmful blue-green algae, which are capable of transporting itself in the vertical direction in the water column. The available validation data for Utah could only validate presence of algae at few sites and time windows. This was the main reason for choosing Lake Utah to formulate hypotheses and not to produce concrete results. Guided by the hypotheses formulated by the descriptive analysis of the Utah case study, Paterswoldsemeer C-SAR image analysis was more methodological and less exploratory.

The existing literature on algae detection has used data from satellites like ERS-2 and ENVISAT (Bresciani, et al., 2014; Wang et al., 2015). These two satellites are not in operation now (also the spatial resolution was around 30 m and the revisit time varied from 35 to 40 days), hence they were unfit for the current research. The validation data in their study is quasi-synchronized optical data. Lack of good quality optical images has stretched their study period to years. In this study, however, there was an ambition of sensing one complete growth cycle of an algal bloom. Availability of in-situ measurement for the period made it the primary source of validation data. The optical data is also included but seldom found to be in sync with radar data.

5. 2 Methods used in the study

Radar image processing was a challenging task. The use of open and relatively young software (SNAP) brought additional issues of an ever changing software environment. In this study standard preprocessing steps were used. The one of the issue with SAR images is its inherent speckle noise. Studies have shown that better handling of speckle in radar images can improve the results (Lee et al., 1994). For Utah a standard speckle filter was applied to remove speckle. But, for Paterswoldsemeer the need for high spatial resolution reduced the alternatives to refined lee speckle filter (this filter does not degrade the spatial resolution). Additionally, resampling of data with a bilinear interpolation function was done to prepare the final processed images of this site. During analysis the use of a window further reduced speckle noise by means of taking the window average. These processed may have caused loss of some information.

Bresciani et al., 2014 in their paper on monitoring algae in Curonian Lagoon used CMOD model to remove the effect of wind from the water backscatter (Section 2.5). This study was preceded by the study where one of the authors tested the application of CMOD for the Lagoon (De Carolis, Parmiggiani, & Arabini, 2004). In this study, CMOD model could not be applied as the model first creates a land mask. The SRTM DEM is used to create the mask. The lakes were identified as land surface in the current version of CMOD in SNAP. Besides, the use of CMOD has its own limitations as the model does not produce reliable results for wind speed lower than 5 m/s (Bresciani, et al., 2014; De Carolis, Parmiggiani, & Arabini, 2004)**.**

5. 3 Discussion on the results

The study partly confirmed the results of previous studies. While the goal of the study was to test hypotheses from the first study site at the second one, the second study site further added to the list of research questions. This section is divided in two sub-section to discuss individually the results of the two sites.

5.3.1 Discussion on Lake Utah results

Overall it has been seen that radar backscatter for lakes is predominantly related to wind sheer stress experienced at the surface. However, radar backscatter for lake Utah also presented the influence of surrounding topography. The results from lake Utah agree with the literature on algae sensing in C-SAR imagery. Images experiencing moderate wind stress showed dampening in the regions that were known to suffer from algal blooms.

The lake Utah was known to suffer from intense algal blooms for the month of July. The C-SAR images were available for dates 4, 11, 21 and 28 of July. High temporal resolution of Sentinel-1 provided an opportunity to study the algal bloom at a good temporal scale. The validation data for this period were available from the first instance of reporting of the bloom. This took place on 14 July, but this may only mark the surfacing of the bloom as scums. The extent of the spread and exact beginning of the bloom is missing and incomplete as the algae concentration maps provided information for specific sites. The literature has shown that the bloom may grow at sub-surface level in lakes before it shows up at the surface (Medrano, 2014). The wind speed recorded at the Provo weather station for the dates 4 and 11 July were 11 and 7 m/s, respectively (Fig. 9 and Fig. 11). The two images do not show any variation in regions with high algal concentration that may highlight the suffered region. However, both images show dampening in the southern part of the lake near Mosida. There was no sampling data from the Utah government to confirm the presence of a bloom at Mosida for these dates.

For 21 July, the areas suffering from algae blooms show up in the image as small dampened spots. The wind speed recorded at the station was 5 m/s. At Mosida, the optical image shows infestation of algae and the C-SAR image shows a dampened region that is spread across the similar extent. But this large scale dampening could also be a result of wind shield effect from Eagle mountain in addition to with algae infestation (Fig. 13). This is an interesting case, if understood in light of the result of the Lake Taihu study (Wang et al., 2015). The paper concludes that dampened area caused by wind shields are much larger than the dampening caused by algae infestation. But in this case, large scale dampening may have easily been a result of algal bloom. Their threshold for a dampened region to be classified as algae bloom was set to 10 km^2. It should be noted that their study is empirical in nature and the size of

Lake Taihu is more than 20 times the size of lake Utah. Therefore, this figure needs verification and re-evaluation. As in case of a massive bloom the whole dampened region may very well be caused by bloom.

The chlorophyll distribution (proxy for algal bloom) derived from optical imagery of Sentinel-2 from 22 July, 2016, however, shows a high concentration of algae around the site on 21 July. It can be hypothesized that the dampening in the south observed in the C-SAR images from 4 and 11 July was caused by algal blooms. Under high wind stress, it is possible that the bloom present in the south of the lake spread across the whole lake, thus spreading to more than 90 percent of the lake. Also, the events at Lindon Marina may also be of interest. The samples from 14 till 20 shows the presence of blooms (Fig.12) and the C-SAR image has dampening in the region around Lindon Marina on 21 July (Fig.13). But the optical image from 22 July does not show presence of bloom at the location. The ability of bloom to move as a unit in space may provide a reasoning for this change of location of algal bloom infestation. The integration of algal growth dynamics with that of environmental conditions and information in C-SAR and optical images provide optimistic view to the future of remote sensing of algae in lakes. However, the lack of validation data raises skepticism and desperate need for verification of this interpretation.

For 28 July the recorded wind speed at the station was 4 m/s with changing wind directions. Usually, at the time of changing weather conditions the lake shows dampening of wave breaking and swirls along its borders. However, this did not appear in this image. There could be other reasons for the absence of effects from changing wind conditions, but one of the possible reasons could also be the presence of scums in the lake. The algae may have prevented the formation or development of waves along the coast. However, this cannot be said with certainty as there is no verification data available for this date.

Lastly, the image from 14 August was also interesting as it has strong similarity with the image from 21 July. There is dampening in places with high algae concentration, but visibility of algae in the absence of wind stress is questionable. The literature has shown that the bathymetry can affect the C-SAR signal, but the bathymetry could only explain the north part of the image.

5.3.2 Discussions on Lake Paterswoldsemeer results

Lake Paterswoldsemeer could not confirm most hypotheses produced by analyzing Lake Utah. The quantitative results showed a close relation of backscatter with wind speed, but no dampening was observed in the regions suffering from algal blooms. The surface structure of lake Paterswoldsemeer did not show any patterns as they were seen in case of Lake Utah.

This could be a result of several reasons. First of all, lake Paterswoldsemeer has many islands and channels. This means that the lake has a small fetch, meaning less open area for wind to interact with the surface without being affected by the surroundings and borders. Secondly, the lake has an increase in economic and recreational activities in the months of June, July and August. People visit the lake a lot during the summer (personal communication with the expert of the local water authority). Lastly, the northern regions, which were most affected by algal blooms have more similarity to a narrow channel than to an open lake. The borders of the northern part of the lake are densely populated. It is possible that the increase in backscatter during June till August at sites of algal infestation is caused by the presence of many boats along the edges of the lake. It can be hypothesized that size of the lake plays an important role in development of Bragg waves. When many obstacles are present on the lakes surface and surrounding, the wind field does not stabilize[7]. The wind therefore losses the domination in influencing the backscatter from the surface of lakes and other factors come to play. For lake Utah the long fetch led to wave development, which were then dampened by the presence of algae.

It should also be noted that in the methodology, the meteorology data for Paterswoldsemeer was taken from the weather station at airport Eelde, which is a few kilometers away from the lake and from the weather station placed on the south-eastern edge of the lake. The data from weather station on the lake was given a preference over the data from weather station at Eelde. This data was mostly available for the months of June and July. It is possible that weather station at the lake was measuring local wind stress and not a stabilized wind stress. And on the other hand, it is possible that the wind conditions measured

---

[7] A stabilized wind stress is an unchanging stress from the surrounding objects across the surface area. It may not be the same across the surface but it is steady and dominant.

by the Eelde weather station were stabilized wind stress as the airport has a vast open area. If this is the case, then this has an impact on the wind results. This difference may have led to the shift in relation of backscatter with the wind speed for the three test sites. There may be multiple reasons preventing the development of stable wind stress on the lake.

The wind shield effect on this lake is much less severe than for Utah, as the lake is only surrounded by trees and houses. There are no large geographic features like mountains present around the lake. The effect of wind shield from trees is not be observed in C-SAR images of the lake. The figure 29 shows the lake at two different dates, 31 January 2016 when the wind speed was 6 m/s and 17 July 2016 when the wind speed was 4 m/s. On both instances, the wind was blowing from direction between South and West. But no impression of wind direction is seen in the C-SAR image. The increase in wind stress is manifested as increase in overall backscatter.

The increase in human activity on the lake interfered with the signal from the lake surface. Not only the backscatter at WISP stations was higher, but also the mean backscatter for the time of algae infestation was higher than the mean backscatter from the time when the lake did not suffer from algae. More first-hand knowledge of the state of the lake at the time of image acquisition is needed to make firm conclusions about algal visibility at such sites. Absence of a strong wind field on the surface could have led to the increase in influence of other (unknown) factors on the lake. For example, the effect of local features such as bird population or a small boat is more pronounced in the absence of strong and stable wind stress.

Both lakes sustain large bird populations. Therefore, it is possible that the water surface is disturbed by the movement of birds on the water surface. At the author's visit to lake Paterswoldsemeer, motion of birds on the water surface was observed (Fig. 30). It was concluded that it did not cause much interference to the waves under the conditions of high wind sheer stress. At the time of capture of the image, the wind was blowing from South West at more than 3 m/s and witnessed a gust of 7 m/s in the last fifteen minutes. Therefore, the local interference from the birds' motion was ignored for both study sites. The birds themselves were also ignored because of their small size.

Sources: Esri, HERE, DeLorme, Intermap, increment P Corp., GEBCO, USGS, FAO, NPS, NRCAN, GeoBase, IGN, Kadaster NL, Ordnance Survey, Esri Japan, METI, Esri China (Hong Kong), swisstopo, MapmyIndia, © OpenStreetMap contributors, and the GIS User Community

8

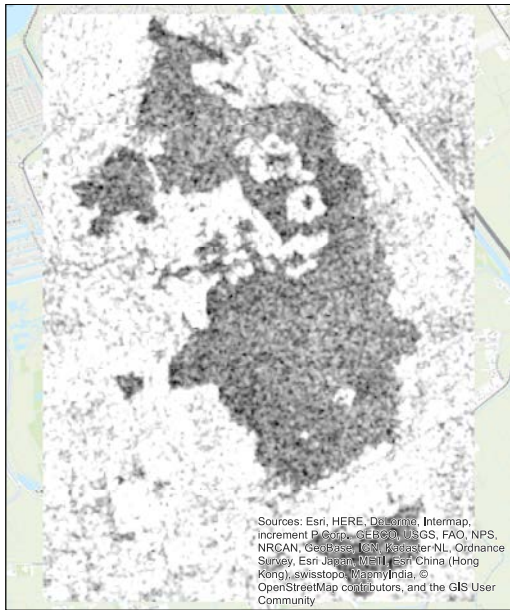| 0 | 285 | 570 | 1,140 |
Meters

Figure 29 Wind field stress from two different wind speeds for Lake Paterswoldsemeer

Overall, lake Paterswoldsemeer provided a much more complicated overview of the lake in the C-SAR image as compared to lake Utah. This can be linked to the small size, short fetch and increase in recreational activity on the lake.

Figure 30 Birds floating in the Lake Paterswoldsemeer

Chapter 6: Conclusions

This study was conducted to explore the use of Sentinel-1 C-band SAR images for sensing algae in lakes. Some research results agree with the current understanding of radar remote sensing of a water body. Besides this, the study also succeeded in putting forward possible factors that affect the backscatter in lakes. Overall, the research has contributed in testing and building knowledge for C-band SAR images of lakes.

Conclusions of the research are given below:

I. What are the factors that cause change in the C-band SAR signal of a lake's water surface?

Wind stress on lake's surface is the most dominant factor that determines C-band SAR signal received from the lake. In addition, the signal is dependent on the physical conditions of lake. These include lake size, bathymetry and surrounding topography. Probably, human activities such as recreational boating also influence the recorded backscatter.

II. Which of these factors support the visibility and detection of algae in a SAR image?

A fully developed wind stress over the lake's surface has a direct effect on the visibility of algae in C-band SAR images. Attenuation in the signal caused by the wind stress in lakes is one way to detect an algal bloom in lakes.

This study also produced some research questions for future researchers about the factors that enhance the detection of algae in C-band SAR images.

a. The size of the lake directly affects the visibility of algae as it is linked to the development of a stabilized wind stress over a lake's surface.

b. For some lakes where waves break or swirl at the shore, in the presence of changing wind stress, the resistance to wind breaking at the edges may also support the visibility of algae.

c. For smaller lakes, large scale human activities on the lake decreases the visibility of algae as it is hard to distinguish human activities from other factors that cause backscatter.

Chapter 7: Recommendations

This research has produced some interesting results and has shown potential in the future of radar remote sensing of algae in lakes. Based on this study. The following is recommended for future studies:

a. This study has shown that many factors contribute to backscatter signal in case of lakes. There is need to locate most of these factors in order to successfully remove the change from those factors in the image. For example, it is observed in this study that human activities influence the backscatter signal. Therefore, for future studies it would be beneficial to have an overpass time during early morning in order to remove the effect of recreational activity.

b. It is also seen in this study that the size of a lake is a crucial element in sensing algae in lake. A lake with surface area of a few hundred km^2 was shown to be suitable of radar remote sensing. Perhaps it would be useful to perform research on a lake with surface area of tens of km^2 to see the gradual increase in complexity with decreasing size of a lake.

c. There is need to perform better processing of C-band SAR images, in particular, the speckle filtering. Research is needed to find the most suitable method of speckle filtering for radar images of a water surface. For example, the signal produced by water surface is due to the waves, the wave crest reflects higher than the trough. This rhythmic high and low backscatter at cm-scale has to be carefully separated from the random speckles in SAR images. It is especially true for small lakes as the waves do not develop in a particular direction (as oppose to a fully developed wave pattern from high wind stress in larger lakes which is easier to quantify, see point below).

d. The relationship between wind speed and C-band backscatter for the first time was quantified using model called CMOD in the twentieth century. These models were primarily built for ocean and sea surfaces, where wind hits the surface uninterrupted by local structures. There is need to re-create these models for lakes so that they accommodate for the impact of wind direction and the surrounding topography. Also, before such a model is applied to a water body, it is advised to test the model application for the water body as done by (De Carolis, Parmiggiani, & Arabini, 2004) before the study of (Bresciani, et al., 2014).

e. This research was hindered by the presence of factors other than the well understood impact of wind stress on the water surface. The potential of using multi-polarized images to filter some of such factors on the water surface should be tested. There is certainly a need to understand the impact of boats for smaller lakes.

f. The current results can also be validated using optical satellite images from various sources. Lake Utah has proved to be an interesting study site for the purpose of sensing algae. A long term research may be combined with optical data, in-situ data and expert knowledge of all the activities occurring on the lake. For example, the concentration map of 20 July (Fig. 12) showed algae at Lindon Marina, which was also seen in C-SAR image from 21 July (Fig. 13) but the optical image from 22 July (Fig.14) showed a different picture. The bloom had moved from Lindon marina to the south of Utah state park. Therefore, synergy of C-SAR with optical and in-situ data may be important for future investigations. A complete picture of occurrence of incidents on the lake may produce interesting findings/ impact of interventions or change in weather conditions.

g. For studying smaller and interconnected lakes, the in-situ data needs to be more extensive to be able to provide a complete picture of the changes. Geo-statistics can be used to convert point data to continuous data. For lake Paterswoldsemeer, which is interconnected to an integrated canal system in the Netherlands. It was observed in this study that a combination of forces interfered with the stress caused by wind. They were probably dependent on lake connectivity with other water bodies like canals or river inlet/outlet and changes in temperature. Therefore, understanding of hydrodynamics of connected water systems may be stressed in the future studies.

Bibliography

Álvarez, S., Antón, X., Labarta, U., Fernández, R., María, J., Figueiras, F. G., . . . Cabanas., J. M. (2008). Renewal time and the impact of harmful algal blooms on the extensive mussel raft culture of the Iberian coastal upwelling system (SW Europe). *Harmful Algae, 7*(6), 849-855.

Anderson, D., Glibert, P., & Burkholder, J. (2002). Harmful algal blooms and eutrophication: Nutrient sources, composition, and consequences. *Estuaries, 25*(4), 704–726.

Attema, W. (1991). The active microwave instrument on-board the ERS-1 satellite. *Proc. IEEE, 79*, 791–9.

Barale, V., Gower, J., & Alberotanza, L. (2010). *Oceanography from Space.* Springer Netherlands.

Barrick, D. E., & Peake, W. H. (1968). A Review of Scattering from Surfaces with Different Roughness Scales. *Radio Sci. , 3*, 865-868.

Beckmann, P., & Spizzichino, A. (1963). *The Scattering of Electromagnetic Waves from Rough Surfaces.* New York, N.Y., 503: Macmillan Co.

Bern, T. I., Wahl, T., Anderssen, T., & Olsen, R. b. (4–6 November de 1992). Oil spill detection using satellite based SAR: Experience from a field experiment. *1st ERS-1 Symposium*, (pp. 829–834). Cannes, France.

Brekke, C., & Solberg, A. H. (2005). Oil spill detection by satellite remote sensing. *Remote sensing of environment, 95*, 1-13.

Bresciani, M., Adamo, M., Carolis, G. D., Matta, E., Pasquariello, G., Vaičiūtė, D., & Giardino, C. (2014). Monitoring blooms and surface accumulation of cyanobacteria in the Curonian Lagoon by combining MERIS and ASAR data. *Remote Sensing of Environment , 146* , 124-135.

Bricaud, A., Bosc, E., & Antoine, D. (2002). Algal biomass and sea surface temperature in the Mediterranean Basin: Intercomparison of data from various satellite sensors, and implications for primary production estimates. *Remote Sensing of Environment, 81*(2), 163-178.

Carolis, G. D., Parmiggiani, F., & Arabini, E. (2004). Observations of wind and ocean wave fields using ERS Synthetic Aperture Radar imagery. *International Journal of Remote Sensing, 25*(7-8), 1283-1290.

Carrara, W., Goodman, R., & Majewski, R. (1995). *Spotlight Synthetic Aperture Radar Signal Processing Algorithms.* Boston, MA: Artech House.

Chorus, I., & Bartram, J. (1999). *Toxic cyanobacteria in water: a guide to their public health consequences, monitoring and management.*

Cutrona, L. (1990). Synthetic aperture radar. Em *Radar handbook 2* (pp. 2333-2346).

Cutrona, L. J., Vivian, W. E., Leith, E. N., & Hall, G. O. (April de 1961). A High Resolution Radar Combat-Surveillance System. *IRE Trans., MIL-5*, 127-131.

Dall'Olmo, G., & Gitelson, A. A. (2005). Effect of bio-optical parameter variability on the remote estimation of chlorophyll-a concentration in turbid productive waters: experimental results. *Applied optics, 44*(3), 412-422.

De Carolis, G., Parmiggiani, F., & Arabini, E. (2004). Observations of wind and ocean wave fields using ERS Synthetic Aperture Radar imagery. *International Journal of Remote Sensing, 25*(7–8), 1283–1290.

De Vries, F. P. (1998). *Speckle reduction in SAR using various multi-look techniques.* TNO Physics and Electronic Laboratory. The Hague: TNO report.

Doerffer, R., & Schiller, H. (2007). The MERIS Case 2 water algorithm. *International Journal of Remote Sensing , 28*(3-4), 517-535.

Duan, H., Ma, R., & Hu, C. (2012). Evaluation of remote sensing algorithms for cyanobacterial pigment retrievals during spring bloom formation in several lakes of East China. *Remote Sensing of Environment , 126*, 126-135.

ESA IAP, CyMoNs. (2015).

Fung, A. K., & Chart, H. (1969). Backscatteriuguf Waves by Composite Rough Surfaces. *IEEE Truns. , 17*, 590-597.

Gardner, W. D., Mishonov, A. V., & Richardson, M. J. (2006). Global POC concentrations from in-situ and satellite data. *Deep Sea Research Part II: Topical Studies in Oceanography, 53*(5), 718-740.

GLaSS, D. 5. (2015). *Global Lakes Sentinel Services: WFD reporting case study results: D 5.7.* EU project deliverable, D5.7, SYKE, WI, EOMAP, BC, CNR, TO, BG.

GLaSS, D. 5. (2015). *Shallow lakes with high eutrophication and potentially toxic algae.* TO, SYKE, WI, CNR, BC, VU/VUmc. Global Lakes Sentinel Services, D5.2.

Government, U. (2016). *Utah lake state park*. Obtido em September de 2016, de https://stateparks.utah.gov/parks/utah-lake/

Gower, J. F. (Ed.). (2013). *Oceanography from space* (Vol. 13). Springer Science & Business Media,.

Greeson, P. E. (1969). Lake Eutrophication - A natural Process. *Journal of the American Water Resources Association , 5*(4), 16-30.

Han, J., McCarthy, E. D., Calvin, M., & Benn., M. H. (1968). Hydrocarbon constituents of the blue-green algae Nostoc muscorum, Anacystis nidulans, Phormidium luridium and Chlorogloea fritschii. *Journal of the Chemical Society C: Organic*, 2785-2791.

Hansson, L.-A. (1988). Effects of competitive interactions on the biomass development of planktonic and periphytic algae in lakes. *Limnology and Oceanography , 33*(1), 121-128.

Hasselmann, K. (1972). The Energy Balance of Wind Waves and the Remote SensingProblem. *Proc. Sea Surface Topography from Space, Nat. Oceanic and Atmospheric Admin. tech. Rep. , ERL-228 .*

Heisler, J. P. (2008). Eutrophication and harmful algal blooms: a scientific consensus. *Harmful algae , 8*(1), 3-13.

Hering, D., Borja, A., Carstensen, J., Carvalho, L., Elliott, M., Feld, C. K., . . . Solheim, A. L. (2010). The European Water Framework Directive at the age of 10: a critical review of the achievements with recommendations for the future. *Science of the total Environment, 408*(19), 4007-4019.

Hovland, H. A., & Digranes, G. (1994). Slick detection in SAR images. *IGARSS , 4*, 2038–2040.

Hwang, P. A. (2012). Foam and roughness effects on passive microwave remote sensing of the ocean. *IEEE Transactions on Geoscience and Remote Sensing , 50*(8), 2978-2985.

Ishizaka, J., Sathyendranath, S., & Platt, T. (2010). Ocean Color Contribution To Geo. *Symposium on Remote Sensing and Fisheries*, *15*, p. 17.

Ji, Z.-G. (2008). *Hydrodynamics and water quality: modeling rivers, lakes, and estuaries.*

Jutla, A. S., Akanda, A. S., & Islam, S. (2010). Tracking cholera in coastal regions using satellite observations. *Journal of the American Water Resources Association, 46*(4), 651-662.

Kalmykov, A. I., & Pustovoytenko, V. V. (1976). On Polarization Features of Radio Signals Scattered from the Sea Surface at Small Grazing Angles. *J. Geophys. Res. , 81*, 196&1964.

Keydel, W. (2003). Perspectives and visions for future SAR systems. *IEE Proceedings: Radar, Sonar and Navigation, 50*(3), 97-103.

Kong, F., Ma, R., Gao, J., & Wu, X. (2009). The theory and practice of prevention, forecast and warning on cyanobacteria bloom in Lake Taihu. *Journal of Lake Sciences , 3*, 314-328.

Lee, J.-S., Jurkevich, L., Dewaele, P., Wambacq, P., & Oosterlinck, A. (1994). Speckle filtering of synthetic aperture radar images: A review. *Remote Sensing Reviews , 8*(4), 313-340.

Lehner, S., J., H., W., K., & Rosenthal, W. (1998). Mesoscale wind measurements using recalibrated ERS SAR images. . *Journal of Geophysical Research, 103*, 7847–7856.

Liu, Y., Islam, M. A., & Gao., J. (2003). Quantification of shallow water quality parameters by means of remote sensing. *Progress in Physical Geography , 27*(1), 24-43.

Medrano, E. A. (2014). *Physical Aspects Explaining Cyanobacteria Scum Formation in Natural Systems* . Thesis, Technische Universiteit Eindhoven, Department of Turbulence and Vortex Dynamics , Eindhoven.

Meriluoto, J., & Codd, G. A. (2005). Cyanobacterial monitoring and cyanotoxin analysis. *Acta Academiae Aboensis, 65*(1), 1-145.

Miller, P. I., Shutler, J. D., Moore, G. F., & Groom, S. B. (2006). SeaWiFS discrimination of harmful algal bloom evolution. *International Journal of Remote Sensing , 27*(11), 2287-2301.

O'Brien, H. E., Miadlikowska, J., & Lutzoni, F. (2005). Assessing host specialization in symbiotic cyanobacteria associated with four closely related species of the lichen fungus Peltigera. *European Journal of Phycology , 40*(4), 363-378.

Paerl, H. W., & Huisman, J. (2008). Blooms like it hot. *SCIENCE-NEW YORK THEN WASHINGTON, 320*(5872), 57.

Phillips, 0. M. (1966). *The Dynamics of the Upper Ocean.* Cambridge: Cambridge Univ. Press.

Racault, M.-F., Quéré, C. L., Buitenhuis, E., Sathyendranath, S., & Platt, T. (2012). Phytoplankton phenology in the global ocean. *Ecological Indicators, 14*(1), 152-163.

Reynolds, R. W., Rayner, N. A., Smith, T. M., Stokes, D. C., & Wang, W. (2002). An improved in situ and satellite SST analysis for climate. *Journal of climate, 15*(13), 1609-1625.

Ritchie, J. C., Zimba, P. V., & Everitt, J. H. (2003). Remote sensing techniques to assess water quality. *Photogrammetric Engineering & Remote Sensing, 69*(6), 695-704.

Saxton, J. A., & Lane, J. A. (1952). Electrical Properties of Sea Water. *Wireless Eng. , 291*, 269-275.

Schanda, E. (2012). *Physical fundamentals of remote sensing.* Springer Science & Business Media.

Scheffer, M. (2004). *Ecology of shallow lakes.*

Sellner, K. G. (2003). Harmful algal blooms: causes, impacts and detection. *Journal of Industrial Microbiology and Biotechnology, 30*(7), 383-406.

Shi, J., Yang Du, J., Jiang, L., Chai, L., Mao, K., & al., P. X. (2012). Progresses on microwave remote sensing of land surface parameters. *Science China Earth Sciences , 55*(7), 1052-1078.

Shmelev, A. B. (1972). Wave Scattering by Statistically Uneven Surfaces. *Usp. Fiz. Nauk , 106*, 459-480.

Solberg, A. S. (2004). Automatic oil spill detection based on ENVISAT, RADARSAT and ERS images. *Envisat & ERS Symposium*, (pp. 6-10). Salzburg, Austria.

Soumekh, M. (1999). *Synthetic aperture radar signal processing* (Vol. 7). New York: Wiley, .

Torres, R., Paul, S., Dirk, G., Bibby, D., Davidson, M., Attema, E., & al., P. P. (2012). GMES Sentinel-1 mission. *Remote Sensing of Environment 120*, 9-24.

Ulaby, F., & Lang, D. B. (2015). A strategy for active remote sensing amid increased demand for spectrum. *In Radio Science Meeting (Joint with AP-S Symposium), USNC-URSI, IEEE*, 263-263.

Valenzuela, G. R. (1978). Theories for the interaction of electromagnetic and oceanic waves — A review. *Boundary Layer Meteorology, 13*, 61–85.

Visser, P. M., Passarge, J., & Mur, L. R. (1997). Modelling vertical migration of the cyanobacterium Microcystis. *Hydrobiologia , 349*(1-3), 99-109.

Voronovich, A. G., & Zavorotny, V. U. (2001). Theoretical model for scattering of radar signals in k u-and c-bands from a rough sea surface with breaking waves. *Waves in Random Media , 11*(3), 247-269.

Wagner, W. G., Pampaloni, P., Calvet, J.-C., Bizzarri, B., Wigneron, J.-P., & Kerr, Y. (2007). Operational readiness of microwave remote sensing of soil moisture for hydrologic applications. *Hydrology Research, 38*(1), 1-20.

Wang, G., Li, J., Bing Zhang, Q. S., & Zhang, F. (2015). Monitoring cyanobacteria-dominant algal blooms in eutrophicated Taihu Lake in China with synthetic aperture radar images. *33*(1), 139-148.

Wetzel, R. G. (1983). Attached algal-substrata interactions: fact or myth, and when and how? *Periphyton of freshwater ecosystems*, 207-215.

Woodhouse, I. H. (2006). *Introduction to Microwave Remote Sensing.* Taylor & Francis.

Wright, J. W. (1966). Backscattering from Capillary Waves with Application to Sea Clutter. *IEEE Trans. , 14*, 749-754.

Zimba, P. V., & Gitelson, A. (2006). Remote estimation of chlorophyll concentration in hyper-eutrophic aquatic systems: Model tuning and accuracy optimization. *Aquaculture , 256*(1), 272-286.

Appendix 1a

Table 2 Utah Algal Bloom in News

Validation data	*Algal bloom in news - Utah Provo Bay*
04 Sept	Herald Editorial: When will we wake up
31 Aug	Toxic bloom closes Utah reservoir to fishing and boating
30 Aug	Advisories increased, cyanobacteria counts still high in parts of Utah
25 Aug	Researchers ge $ 1 million to study Utah Lake algae blooms
22 Aug	Two areas increased to warning advisoried in Utah Lake due to algal bloom
17 Aug	Utah County lakes continues to be tested for alge blooms
13 Aug	US agency studies Utah Lake, Great Salt Lake to help detect algae bloom outbreaks
09 Aug	ANother species of cyanobacteria found in Utah Lake, labs testing for possible toxicity
02 Aug	Utah Lake reopend for swmmers
28 Jul	With toxin levels downs, Utah lake reopened for boating
27 Jul	Algae decreasing in Utah Lake but another bloom possible
24 Jul	Herald Editorial: Will those responsible for Utah Lake please stand up
22 Jul	No easy solution to algae blooms on Utah Lake
21 Jul	Health officials: Bizzare foam coming from Bluffdale sewer grate unlikely related to algae
21 Jul	Utah Lake closure sinking business' profits
20 Jul	Utah Division of Water Quality testing Utah Lake waters daily for cyanobacteria
18 Jul	Utah Lake's toxic algae affecting Saratoga Springs secondary water, flowing into Jordan River
16 Jul	At least 8 report illnesses after exposure to Utah Lake "Water with these levels of concentration in the algal bloom pose serious health risks," said Ralph Clegg, executive director of the Utah County Health Department. "To protect the health of people and animals that use the lake, it is necessary for the lake to remain closed until it is safe for recreation."
15 July	Utah Lake shut down According to satellite imagery, the algal bloom covers about 90 percent of the lake on the surface and subsurface
14 July	Report: Half of Utah lakes dont meet water quality standard

Table 3 Information of satellite pass and weather for lake Utah

2016	S1	UTC Time	Provo Bay Time	Path	Weather data available at	Wind Direction
1	30 March	01:26:41	19:26:41	Ascending	4.1 m/s at 6:56 PM and 7:47 PM on 29	SSW
2	16 April	13:33:55	07:33:55	Descending	3.1 m/s at 6:50 and Calm at 7:50 AM @16April	NE
3	23 April	01:26:41	19:26:41	Ascending	7.7m/s at 6:47 and 7.7 at 7:59 PM @ 22 April	SW
4	30 April	01:18:37	19:18:37	Ascending	6.2m/s at 6:48 and 4.6 m/s at 7:47 @29April	SW & WSW
5	05 May	01:26:48	19:26:48	Ascending	3.1m/s at 7:47 and 4.1 m/s at 8:47 @ 04 May	WNW & ESE
6	10 May	13:33		Descending	2.1 m/s at 6:47 AM. calm weather conditions at 7:47 AM	variable
7	24 May	01:18		Ascending	2.1 m/s at 6:47 PM and at 7:47 PM.	WNW to variable
8	3 June	13:33		Descending	calm at 6:49 AM to low wind speed of 1.5 m/s	East
9	10 June	01:26	19:26:44	Ascending	6.2 m/s at 7:48 and 6.2 m/s at 8:47 @ 9 June	SW &WNW
10	4 July	01:26:45		Ascending	11m/s from 6:48 PM till 7:48 PM on 3 July at Provo.	S
11	11 July	01:18:44		Ascending	7m/s from the direction West North West from 6:47 PM to 7:47 PM	West North West
12	21 July	13:34:04		Descending	4.1m/s at 6:49 AM to 6.2m/s at 7:49 AM	ESE
13	28 July	01:26:44	19:26:44	Ascending	3.6 m/s at 7:47 and Calm at 8:47 @27 July	W & Calm
14	14 Aug	13:34:02	07:34:02	Descending	Calm at 6:47, 7:47 and 8:47	Calm

Appendix 1b

Table 4 Information on location of weather station, satellite pass and weather conditions for lake Paterswoldsemeer

Date 2016	Degree Latitude	Degree Longitude	Wind direction	Wind speed	Temp_air		Pass
31-1	53.128487	6.585829	240	6.2	4	6:49:00 AM	D
3-2	53.128487	6.585829	265	4.6	4	6:24:00 PM	A
7-3	53.128487	6.585829	200	2.1	-1	6:49:00 AM	D
22-3	53.128487	6.585829	315	4.1	7	6:24:00 PM	A
30-5	53.128487	6.585829	0		17.6	7:49:00 AM	D
2-6	53.128487	6.585829	358.5	2.82	15	7:24:00 PM	A
11-6	53.128487	6.585829	184.8	1.24	13.5	7:49:00 AM	D
30-6	53.128487	6.585829	190	2.4	14.2	7:41:00 AM	D
5-7	53.16346	6.577617	237.1	1.85	16.4	7:49:00 AM	D
15-7	53.16346	6.577617	262.25	3.3	16.5	7:16:00 PM	A
17-7	53.16346	6.577617	261.0333	3.93	18.1	7:49:00 AM	D
20-7	53.16346	6.577617	157.4	2.45	23.8	7:24:00 PM	A
24-7	53.16346	6.577617	302	1.35	18.6	7:41:00 AM	D
27-7	53.16346	6.577617	211.4	1.7	17.5	7:16:00 PM	A
1-8	53.128487	6.585829	265	4.1	18	7:24:00 PM	A
10-8	53.128487	6.585829	245	1.5	9	7:49:00 AM	D
13-8	53.128487	6.585829	245	5.1	18	7:24:00 PM	A
22-8	53.128487	6.585829	200	5.1	15	7:49:00 AM	D
6-9	53.128487	6.585829	180	1	22	7:24:00 PM	A
15-9	53.128487	6.585829	90	3.6	17	7:49:00 AM	D
18-9	53.128487	6.585829	0	2.1	12	7:24:00 PM	A
9-10	53.128487	6.585829	499	0.5	5	7:49:00 AM	D